Discovery of 3-[2-(Imidazo[1,2-*b*]pyridazin-3-yl)ethynyl]-4-methyl-*N*-{4-[(4-methylpiperazin-1-yl)methyl]-3-(trifluoromethyl)phenyl}benzamide (AP24534), a Potent, Orally Active Pan-Inhibitor of Breakpoint Cluster Region-Abelson (BCR-ABL) Kinase Including the T315I Gatekeeper Mutant

Wei-Sheng Huang,* Chester A. Metcalf, Raji Sundaramoorthi, Yihan Wang, Dong Zou, R. Mathew Thomas, Xiaotian Zhu, Lisi Cai, David Wen, Shuangying Liu, Jan Romero, Jiwei Qi, Ingrid Chen, Geetha Banda, Scott P. Lentini, Sasmita Das, Qihong Xu, Jeff Keats, Frank Wang, Scott Wardwell, Yaoyu Ning, Joseph T. Snodgrass, Marc I. Broudy, Karin Russian, Tianjun Zhou, Lois Commodore, Narayana I. Narasimhan, Qurish K. Mohemmad, John Iuliucci, Victor M. Rivera, David C. Dalgarno, Tomi K. Sawyer, Tim Clackson, and William C. Shakespeare

ARIAD Pharmaceuticals, Inc., 26 Landsdowne Street, Cambridge, Massachusetts 02139

In the treatment of chronic myeloid leukemia (CML) with BCR-ABL kinase inhibitors, the T315I gatekeeper mutant has emerged as resistant to all currently approved agents. This report describes the structure-guided design of a novel series of potent pan-inhibitors of BCR-ABL, including the T315I mutation. A key structural feature is the carbon−carbon triple bond linker which skirts the increased bulk of Ile315 side chain. Extensive SAR studies led to the discovery of development candidate **20g** (AP24534), which inhibited the kinase activity of both native BCR-ABL and the T315I mutant with low nM IC$_{50}$s, and potently inhibited proliferation of corresponding Ba/F3-derived cell lines. Daily oral administration of **20g** significantly prolonged survival of mice injected intravenously with BCR-ABL^{T315I} expressing Ba/F3 cells. These data, coupled with a favorable ADME profile, support the potential of **20g** to be an effective treatment for CML, including patients refractory to all currently approved therapies.

Introduction

Chronic myeloid leukemia (CML^a), a hematological stem-cell disorder, is characterized by the occurrence of the Philadelphia (Ph) chromosome, a truncated version of chromosome 22 resulting from the reciprocal translocation between chromosomes 9 and 22. This single mutagenic event leads to the juxtaposition of two genes, whose product is the fusion protein BCR-ABL, a constitutively active tyrosine kinase that drives the pathogenesis of CML.[1] Development of tyrosine kinase inhibitors targeting the BCR-ABL oncogene constitutes an effective approach to treating CML, as demonstrated by the clinical success of imatinib, a potent first generation BCR-ABL inhibitor.[2] In patients with newly diagnosed CML in the chronic phase, daily oral administration of imatinib has demonstrated 89% major cytogenetic response rates and 82% complete cytogenetic response rates. These response rates translated into impressive event-free survival (81%), freedom from progression (93%), and overall survival (86%) rates.[3] Despite the clear benefits of imatinib, many patients eventually develop intrinsic or acquired resistance to this first-line therapy. Resistance rates were reported to be 3−4% per year in newly diagnosed chronic phase CML and much higher with CML patients in accelerated

and blastic phases, with the percentage being 40−50% and 80%, respectively.[4] Mutations in the kinase domain of BCR-ABL that impede effective inhibitor binding are the primary mechanism of acquired imatinib resistance;[5] to date, at least 100 different point mutations have been identified in CML patients who are resistant to this drug.

To overcome resistance in CML, a number of second generation inhibitors have been developed.[6] These include imatinib-like inhibitors nilotinib[7] and bafetinib,[8] and dual SRC/ABL inhibitors dasatinib[9] and bosutinib.[10] Both dasatinib and nilotinib have been approved for the treatment of adults in all phases of CML with resistance or intolerance to imatinib whereas bafetinib and bosutinib are in late-stage clinical testing. Despite the effectiveness of these second-generation compounds to inhibit most imatinib resistant BCR-ABL mutants, subsets of mutants remain resistant. In particular, a common characteristic of these agents is their inability to inhibit the BCR-ABL^{T315I} mutant at the "gatekeeper" position which represents ~15−20% of all clinically observed mutants.[10b,11,12]

To address this unmet need, several programs targeting development of potent BCR-ABL^{T315I} inhibitors have been established and a number of reviews have detailed progress in this area.[13] Briefly, compounds with notable BCR-ABL^{T315I} inhibitory activity include (Figure 1): PPY-A,[14] TG101113,[15] and dual ABL/Aurora inhibitors tozasertib (MK-0457, VX-680),[16] danusertib (PHA-739358),[17] AT-9283,[18] and KW-2449.[19] The dual ABL/Aurora agents have advanced to clinical trials in patients with treatment-resistant CML, in general via intravenous administration. While tozasertib has demonstrated some activity as salvage therapy,[16] clinical development has been halted due to toxicity concerns. Despite this progress, there are presently no approved pharmaceutical therapies for CML patients harboring the BCR-ABL^{T315I} mutation.

---

*To whom correspondence should be addressed. Phone: 617-621-2341. Fax: 617-494-8144. E-mail: wei-sheng.huang@ariad.com.
^{a} Abbreviations: CML, chronic myeloid leukemia; BCR-ABL, breakpoint cluster region-abelson; ADME, absorption distribution metabolism excretion; Src/Abl, sarcoma/Abelson; DFG, aspartic acid-phenylalanine-glycine; AUC, area under curve; PK, pharmacokinetic; Ph+, Philadelphia chromosome-positive; FLT3, FMS-like tyrosine kinase 3; FGFR, fibroblast growth factor receptor; VEGFR, vascular endothelial growth factor receptor; c-Kit, cytokine receptor; PDGF, platelet-derived growth factor; CDK2, cyclic dependent kinase 2; EGFR, epidermal growth factor receptor; FAK, focal adhesion kinase; IGF1R, insulin-like growth factor receptor; JAK2, janus kinase 2; WT, wild type.
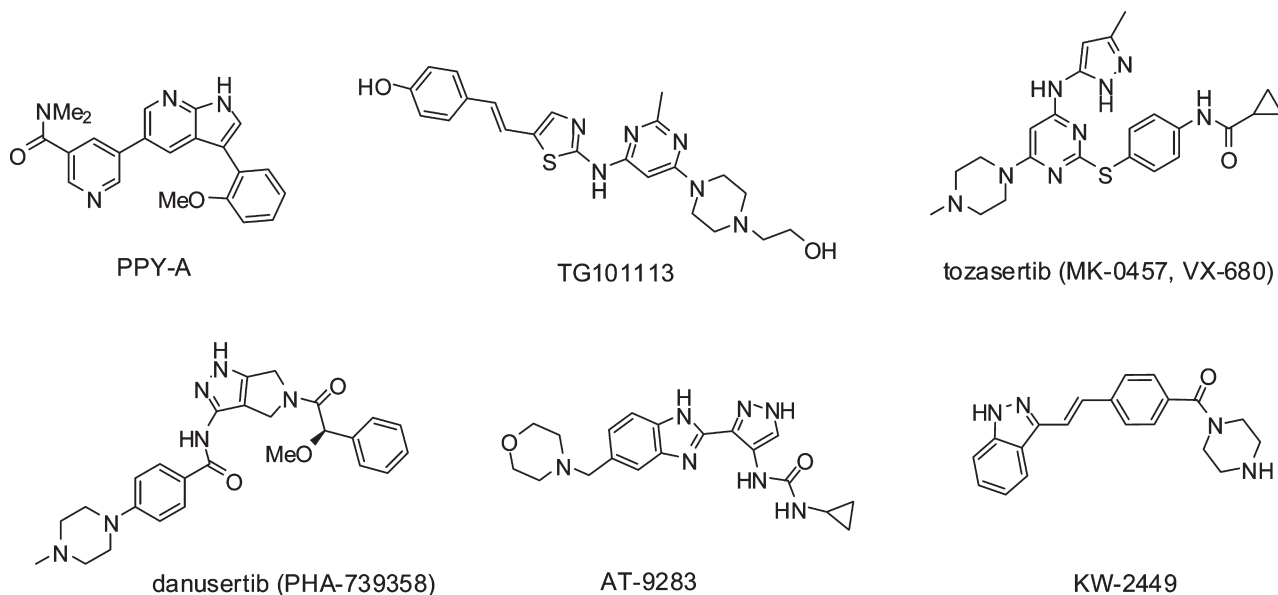
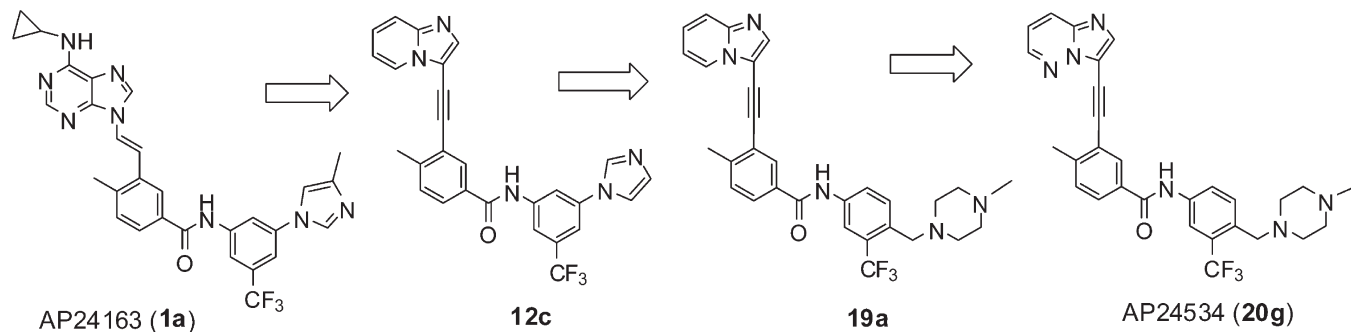**Figure 1.** BCR-ABL[T315I] kinase inhibitors with disclosed chemical structures.

Figure 2. Key medicinal chemistry optimization leading to clinical candidate **20g**.

It is generally believed that next-generation ABL inhibitors capable of exerting a high level of disease control in CML should incorporate potent activity not only against BCR-ABL[T315I] but also the full range of BCR-ABL kinase domain mutations as well as the native enzyme itself. Such a "pan-BCR-ABL" inhibitor would have the potential to treat disease resistant to all current therapies and potentially to suppress the emergence of resistance when deployed at earlier disease stages. Recently, we described the biological characterization of AP24534 (**20g**), a potent, orally available multitargeted kinase inhibitor.[20] **20g** is potently active against BCR-ABL[T315I] and all other tested BCR-ABL variants and suppresses emergence of resistant mutations in a cell-based screen, thereby fulfilling the criteria for a pan-BCR-ABL inhibitor. In this report, we describe the medicinal chemistry and structural design strategy that led to the discovery of this molecule. Key anticipated design aspects included template morphing, exploration of alternate hydrophobic linkers, and considerable SAR around the pendant DFG-out phenyl ring (Figure 2).
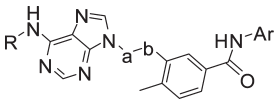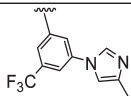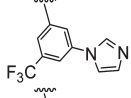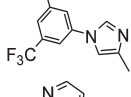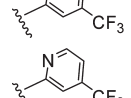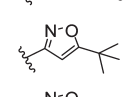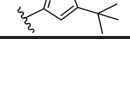
Inhibitor Synthesis

The synthesis of 9-(ethenyl)purine based inhibitors **1a−e** (Table 1) has been reported previously.[21a] The preparation of 9-(ethynyl)purine based inhibitors **6a** and **6b** is depicted in Scheme 1. 9-(Cyclopropylamino)purine **2**, prepared by S_NAr displacement of 6-chloropurine with cyclopropylamine, was deprotonated with sodium hydride then reacted with tetrachloroethene to yield 9-(trichloroethenyl)purine **3**.[22] Exhaustive dechlorination of **3** with *n*-butyllithium followed by quenching with methanol generated terminal alkyne **4**.[22] Subsequent Sonogashira coupling[23] of **4** with iodobenzamide **5** furnished inhibitors **6**, albeit in low yields.

The syntheses of inhibitors **12** bearing C−C≡C−C structural motifs were based on a tandem Sonogashira coupling strategy. Initially, two general methods (A and B) were explored employing either the heteroaryl bromides **7** or the iodobenzamides **5** as coupling partners in the first Sonogashira reaction (Scheme 2). In employing method B, the final coupling reaction between ethynylbenzamides **11** and **7** often afforded low yields of desired products with dimerization of **11** being the major competing reaction. Method A therefore was adopted as the standard approach to **12**. In the second step involving cleavage of the trimethylsilyl group (from **8** to **9**, or **10** to **11**), deprotection with either tetrabutylammonium fluoride or potassium carbonate/methanol worked equally well.

Scheme 3 illustrates the synthesis of inhibitors **12a−e** compiled in Table 2. Starting material *N*-(imidazo[1,2-*a*]pyridin-8-yl)acetamide **13** was prepared by condensing 2,3-diaminopyridine and chloroacetaldehyde diethylacetal followed by acetamidation, according to literature methods.[24] Selective bromination of **13** furnished **7b**, which was hydrolyzed under acidic conditions to yield bromide **7a**. Direct Sonogashira reaction of **7a** with trimethylsilylacetylene failed to afford the desired coupling product but the *N,N*-bis-Boc protected derivative **7a′**

Table 1. Early Structure−Activity Relationships (IC$_{50}$ in nM)

Cmpnd	R	a-b	Ar	ABL kinase	T315I kinase	ABL (Ba/F3)	T315I (Ba/F3)
1a	cyclopropyl	*trans*-CH=CH		25	478	7.3	422
1b	cyclopropyl	*trans*-CH=CH		13	542	4.2	298
1c	H	*trans*-CH=CH		1.6	386	1.4[a]	295
1d	cyclopropyl	*trans*-CH=CH		20	14142	4.8	2746
6a	cyclopropyl	C≡C		30	524	2.0	548
1e	cyclopropyl	*trans*-CH=CH		23	15513	12	7122
6b	cyclopropyl	C≡C		28	359	3.0	513

[a] Measured in K562 cell line.

Scheme 1. Synthesis of 9-(Ethynyl)purine Based Inhibitors[a]
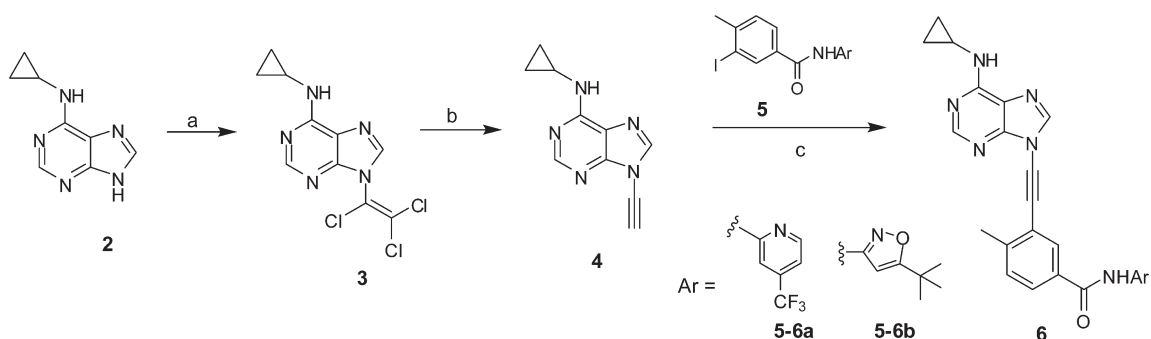
[a] Reagents and conditions: (a) tetrachloroethylene, NaH, HMPA, 60 °C; (b) *n*-BuLi, THF, −78 °C; (c) 5 mol % Pd(PPh$_3$)$_4$, 2.6 mol % CuI, Et$_3$N, Tol, 55 °C.

Scheme 2. General Methods for the Synthesis of Inhibitors
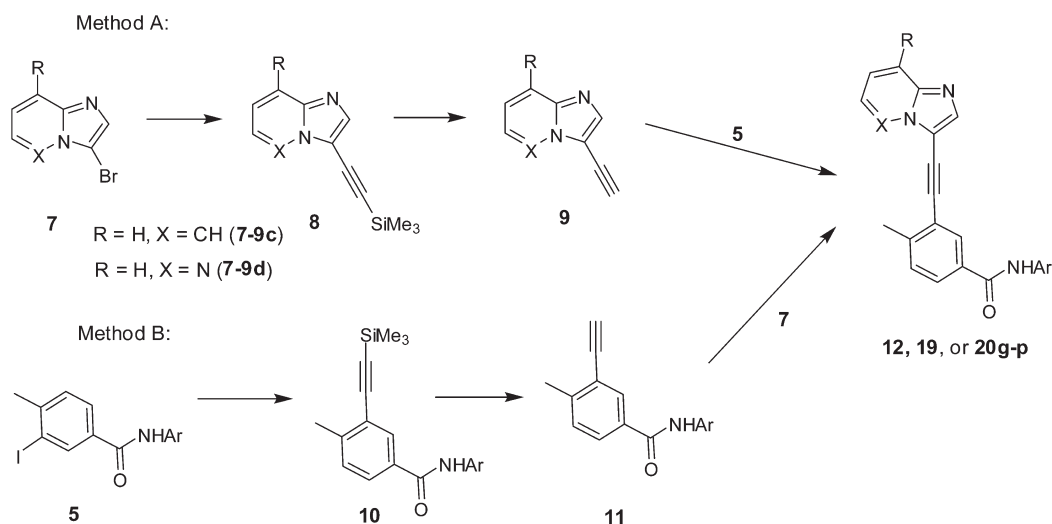
Scheme 3. Synthesis of Inhibitors **12a−e**[a]
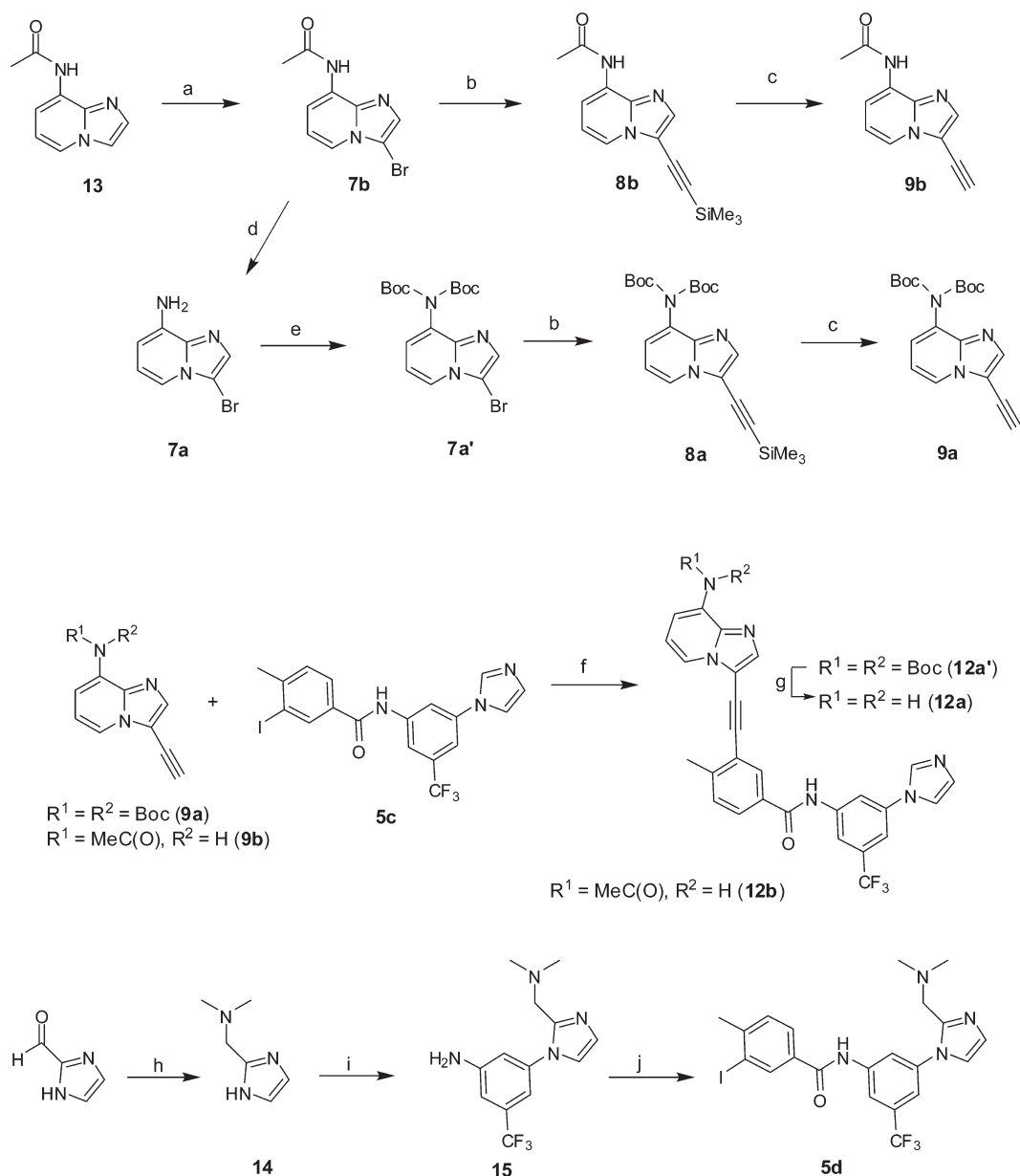
[a] Reagents and conditions: (a) Br$_2$, EtOH, rt; (b) trimethylsilylacetylene, 5 mol % Pd(PPh$_3$)$_2$Cl$_2$, 7.5 mol % CuI, (*i*-Pr)$_2$NEt, DMF, 80 °C; (c) TBAF, THF, rt; (d) conc. HCl, EtOH, reflux; (e) (Boc)$_2$O, cat. DMAP, THF, rt; (f) 5 mol % Pd(PPh$_3$)$_4$, 7.5 mol % CuI, (*i*-Pr)$_2$NEt, DMF, rt; (g) TFA, CH$_2$Cl$_2$, rt; (h) aq Me$_2$NH, NaBH$_4$; (i) 3-bromo-5-trifluoromethylaniline, 15 mol % 8-hydroxyquinoline, 15 mol % CuI, K$_2$CO$_3$, DMSO, 120 °C; (j) 3-iodo-4-methylbenzoyl chloride, (*i*-Pr)$_2$NEt, THF, rt.

underwent smooth coupling. Subsequent desilylation furnished terminal alkyne **9a**, which was coupled with iodobenzamide **5c** to yield **12a′**. Subsequent removal of the Boc protecting groups furnished inhibitor **12a**. For the synthesis of **12d**, 2-imidazole-carboxaldehyde was first reacted with dimethylamine under reductive amination conditions to furnish **14**. Compound **14** was then converted into iodobenzamide **5d** similarly to the preparation of **5c** via a published two-step procedure employing a copper-catalyzed *N*-arylation with 3-bromo-5-(trifluoro-methyl)aniline followed by amide formation with 3-iodobenzoyl chloride.[25] Subsequent Sonogashira coupling of **5d** with **9c** (structure shown in Scheme 2) furnished inhibitor **12d**. Compound **12e** was obtained via the same route as **12d** using 4-imidazolecarboxaldehyde and pyrrolidine as starting materials. Inhibitors **12b** and **12c** were constructed via the standard

three-step protocol outlined in general method A from **9b** and **5c**, or **9c** and **5c**, respectively.

The synthesis of inhibitors **19a−j** (Table 3) followed general method A via Sonogashira coupling of **9c** with the appropriate iodobenzamides. The preparation of **19a** illustrates the general approach (Scheme 4). Thus, 4-nitro-2-(trifluoromethyl)benzyl bromide, prepared from bromination of 4-nitro-2-(trifluoro-methyl)toluene with *N*-bromosuccinimide, underwent S$_N$2 displacement with *N*-methylpiperazine yielding **16a**. Reduction of the nitro group followed by amide bond formation provided the requisite iodide **18a**. Sonogashira coupling of **18a** with **9c** furnished **19a**. Analogues **19d−f** and **19h−j** were constructed via similar routes but with the required commercially available secondary amines as the nucleophile in the initial substitution reaction. Inhibitors **19b**, **19c**, and **19g** were prepared similarly

Table 2. SAR Based on Imidazo[1,2-*a*]pyridine Template (IC$_{50}$ in nM)

12
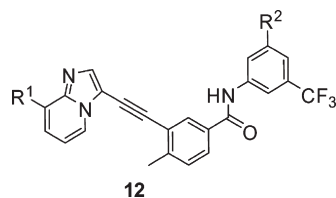
Cmpnd	R^1	R^2	ABL kinase	T315I kinase	ABL (Ba/F3)	T315I (Ba/F3)	Parental (Ba/F3)
12a	H$_2$N—		2.3	1216	8.6	72	10000
12b			6.4	2414	11	44	7392
12c	H		26	102	10	471	9845
12d	H		45	168	11	251	7013
12e	H		26	185	9.4	135	3537

from the coupling of **9c** with **18b**, **18c**, and **18g**, respectively. The requisite benzoic acid precursor[26] to **18b**, the substituted aniline precursor[27] to **18g**, and the iodobenzamide **18c**[28] were all prepared according to published procedures.

In the synthesis of **19k**−**m**, protection of the terminal piperazine nitrogens was necessary due to increased reactivity toward aroyl chloride relative to the anilino NH in the amide formation step; this is illustrated in Scheme 5. Iodobenzamide **18l** was prepared similarly to **18a** using *N*-Boc-piperazine instead of *N*-methylpiperazine as the starting nucleophile. Deprotection of **18l** and subsequent alkylation with 1-bromo-2-fluoroethane furnished **18k**. In the preparation of **18m**, a Boc group was first introduced onto **16m**, which was prepared via regiospecific *N*-alkylation of the less sterically hindered NH of 2-methylpiperazine with 4-nitro-2-(trifluoromethyl)benzyl bromide. Elaborated **16m′** was then converted into iodide **18m** in a manner similar to **18a**. Sonagashira coupling of Boc-protected iodides **18l** or **18m** with **9c** and subsequent deprotection furnished inhibitors **19l** and **19m**, respectively.

Synthesis of inhibitors **20a**−**p** (Tables 4 and 5) followed the Sonagashira coupling strategy generally outlined in method A. All starting heteroaryl bromides were obtained from commercial sources, and the corresponding iodobenzamides were prepared from the requisite acids and anilines via chemistry discussed previously, with the exception of aniline precursor **17o** (Scheme 6). **17o** was synthesized via S$_N$2 substitution of 2-bromo-4-nitrobenzyl bromide with *N*-methylpiperazine, followed by Suzuki coupling of the corresponding bromide with cyclopropaneboronic acid and subsequent reduction of the nitro group, as shown in Scheme 6. The CH$_2$CH$_2$-linked analogue **24a** (Table 6) was accessed directly via hydrogenation of **20g** and the *trans*-CH=CH-linked inhibitor **24b** (Table 6) was prepared via Heck coupling of styrene **23** (Scheme 7). The latter was obtained from a Stille coupling of **18a** with tributyl(vinyl)tin as depicted in Scheme 7.

Results and Discussion

Compounds were evaluated for their kinase inhibitory activity against both native and mutant (T315I) ABL as previously described.[21a] Their cellular activity was assessed using Ba/F3 cells transfected with native BCR-ABL or BCR-ABL^{T315I} and inhibition of parental, nontransfected Ba/F3 cells was used as a control. Additionally, pharmacokinetic properties for active compounds were evaluated early in rats to help guide series selection.

Early Linker Exploration and Initial Template Morphing. Recently, we described a novel series of potent, orally bioavailable ABL kinase inhibitors based on the 9-[aren(ethenyl)]purine template which target the inactive, DFG-out conformation of the ABL protein.[21] One subtype from this series, exemplified by AP24163 (**1a**, Figure 2) and its des-methyl and des-cyclopropyl analogues **1b** and **1c** (Table 1), demonstrated modest potency against BCR-ABL^{T315I} in both biochemical and cell-based assays (IC$_{50}$s = 300−500 nM) in addition to potently inhibiting native BCR-ABL.[21a] It is noteworthy that **1a**−**c** inhibit ABL^{T315I} because the structurally similar nilotinib is completely inactive against this mutant. When nilotinib is docked into the model of ABL^{T315I} kinase, there is an obvious steric clash between the amino group on the pyrimidine ring and the larger gatekeeper isoleucine.[29] This steric repulsion, in combination with a forfeited hydrogen bond between the amino group and the hydroxyl side chain of threonine observed in the imatinib:ABL cocrystal structure (PDB: 1IEP), severely impaired the preferred ligand−protein interaction, impeding binding and rendering both imatinib and nilotinib inactive toward the ABL^{T315I} mutant.[29−32] Such a clash is not observed in the model of **1a** when docked into the ATP-binding pocket of ABL^{T315I} due to the less sterically demanding vinyl linkage (Figure 4), which may in part explain increased activity of **1a**−**c** against ABL^{T315I}.

The activity of the 9-[aren(ethenyl)]purine series toward ABL^{T315I} stimulated further exploration of an alternate,

Table 3. B-Ring SAR around Inhibitor **19a** (IC$_{50}$ in nM)

| Cmpnd	R^1	R^2	ABL kinase	T315I kinase	ABL (Ba/F3)	T315I (Ba/F3)	Parental (Ba/F3)
19a	*(N-methylpiperazinylmethyl)*	H	9.0	56	3.6	26	1567
19b	reverse amide of **19a**, R^1 and R^2 identical		9.0	89	2.0	50	1800
19c	H	*(N-methylpiperazinylmethyl)*	24	206	11	232	5381
19d	*(morpholinylmethyl)*	H	78	668	2.1	727	7444
19e	*(dimethylaminopyrrolidinylmethyl)*	H	15	92	5.4	58	812
19f	*(N-methyl-1,4-diazepanylmethyl)*	H	13	107	8.4	157	1876
19g	*(methoxypiperidinylmethyl)*	H	9.1	83	3.4	77	1009
19h	*(N-ethylpiperazinylmethyl)*	H	23	157	5.2	49	1946
19i	*(N-isopropylpiperazinylmethyl)*	H	56	219	8.0	43	1646
19j	*(N-(2-hydroxyethyl)piperazinylmethyl)*	H	19	71	2.3	42	1959
19k	*(N-(2-fluoroethyl)piperazinylmethyl)*	H	49	250	4.0	166	971
19l	*(piperazinylmethyl)*	H	14	49	3.5	22	2077
19m	*(methylpiperazinylmethyl)*	H	22	165	9.5	203	3966

less sterically demanding two-carbon atom acetylenyl spacers in the design of inhibitors against this mutant. Incorporation of this rigid, rod-shaped linker should further reduce steric repulsion with the bulk of the isoleucine side chain. As shown in the ABL model (Figure 4), the corresponding 9-[(aren)-ethynyl]purine analogue **1a′** is predicted to bind to the protein in a mode identical to **1a**. All key ligand−protein interactions, including hydrogen bonds, hydrophobic and van der Waals (vdw) contacts are maintained and the acetylene linkage further reduces steric clash with the larger Ile315 residue. This model motivated us to prepare then test two matched sets of molecules (**1d** vs **6a**, **1e** vs **6b**, Table 1) against the ABL^{T315I} mutant. Encouragingly, inhibitors bearing the acetylene linkage were 30−40-fold more potent in enzymatic assays and 5−10-fold more potent in cell-based antiproliferation assays, relative to their vinyl-linked analogues. Despite increased potency against ABL^{T315I}, both 9-[(aren)ethynyl]purine compounds **6a** and **6b** displayed poor pharmacokinetic profiles. When dosed orally in rats, **6a** exhibited low exposure (AUC$_{0−24\,h}$/dose =11.8 ng·h/ mL/mg/kg) and a short half-life ($t_{1/2}$ = 1.5 h). Note this oral exposure is 2250-fold lower than **1d** (compound **9i** from ref 21a),

which displayed higher AUC and C_{max} levels when evaluated previously.[21a] Given the single structural modification between **6a** and **1d** (vinyl vs acetylenyl), we reasoned that it might be very challenging to make orally active inhibitors based on the 9-[(aren)ethynyl]purine template of **6a**. Furthermore, in contrast to the readily accessible 9-[(aren)ethenyl]purines via Heck-type chemistry,[33] preparation of the 9-[(aren)ethynyl]purine core involved low yielding steps which made further SAR exploration with this template impractical.[22]

To overcome the liabilities associated with the 9-[(aren)-ethynyl]purine-based inhibitors, we sought alternate ways to exploit the potency gain exhibited by the acetylene linkage. Instead of pursuing **1a′**, the direct acetylene-linked analogue of **1a** (Figure 3), we targeted inhibitors in which the linker connects the hinge binding template to the N-aryltoluamide subunit via carbon atoms. Such C−C≡C−C structural motifs should be chemically and pharmacologically more stable than the corresponding N−C≡C−C moiety exhibited by the ynamine-like 9-[(aren)ethynyl]purine series and are easily accessed via well-known Sonogashira coupling reactions.[23] Thus, we implemented a template morphing strategy

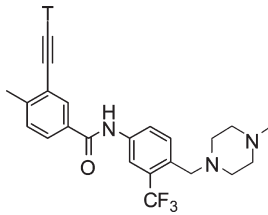**Scheme 4.** Preparation of Inhibitor **19a** and Chemical Structures of **18b**, **18c**, and **18g**[a]
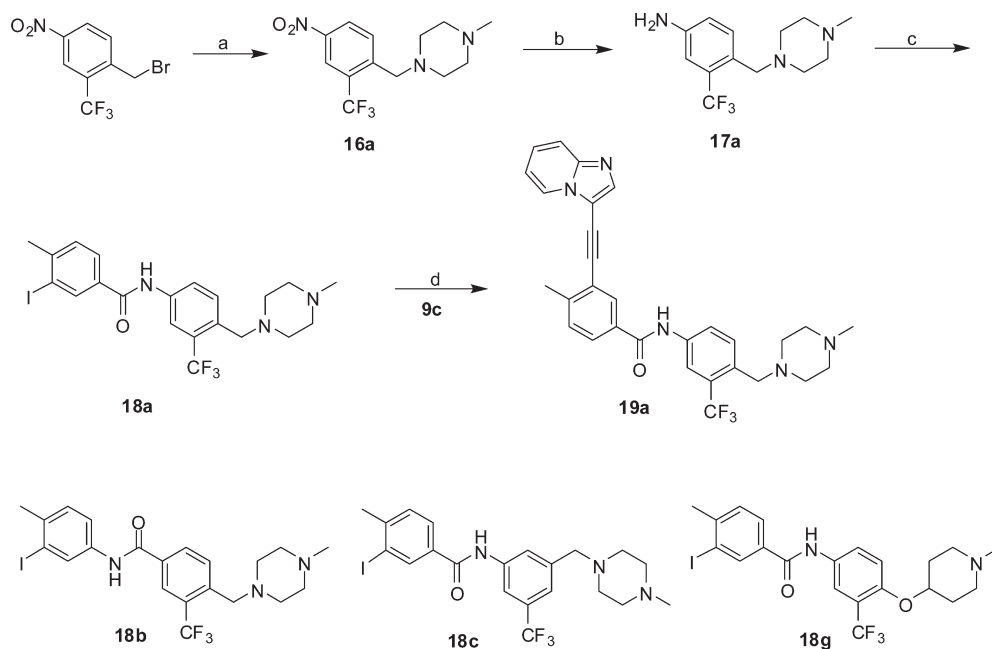
[a] Reagents and conditions: (a) 1-methylpiperazine, Et$_3$N, CH$_2$Cl$_2$, rt; (b) Na$_2$S$_2$O$_4$, acetone/water, reflux; (c) 3-iodo-4-methylbenzoyl chloride, (i-Pr)$_2$NEt, THF, rt; (d) 5 mol % Pd(PPh$_3$)$_4$, 7.5 mol % CuI, (i-Pr)$_2$NEt, DMF, rt.
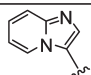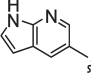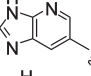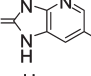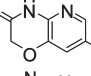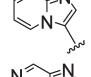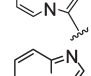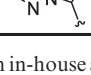
Scheme 5. Synthesis of Inhibitors **19k−m**[a]
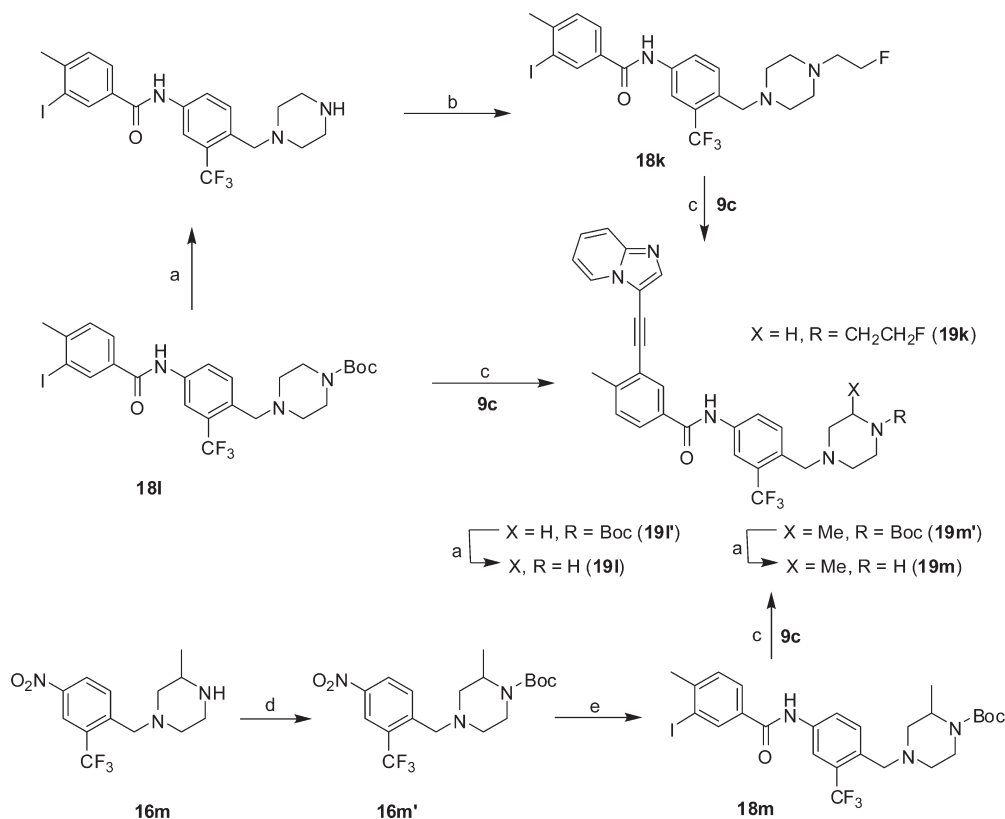
[a] Reagents and conditions: (a) TFA, CH$_2$Cl$_2$, rt; (b) 2-bromofluoroethane, NaHCO$_3$, DMF, 80 °C; (c) 5 mol % Pd(PPh$_3$)$_4$, 7.5 mol % CuI, (i-Pr)$_2$NEt, DMF, rt; (d) (Boc)$_2$O, cat. DMAP, THF, rt; (e) (i) 10% Pd on carbon, 50 psi H$_2$, EtOH, rt, (ii) 3-iodo-4-methylbenzoyl chloride, (i-Pr)$_2$NEt, THF, rt.

initially targeting the 8-amino-imidazo[1,2-*a*]pyridine ring system because 8-NH and N-1 of this template were predicted to form paired hydrogen-bonds with the kinase hinge region. Relative to **1a−c**, the prototype inhibitor **12a** was 4−6-fold more potent against ABL^{T315I} in cells (IC$_{50}$ = 72 nM) while retaining native ABL activity (Table 2), thus validating our template morphing strategy and further highlighting the increased activity of the acetylene linkage toward ABL^{T315I}. Despite the increased cellular potency, **12a** exhibited low oral bioavailability in rats (F = 5.5%) (Table 7). Likewise, the acetamide derivative

Table 4. Exploration of Alternate Hinge Binding Templates (IC$_{50}$ in nM)

Cmpnd	T	ABL kinase[a]	T315I kinase[a]	ABL (Ba/F3)	T315I (Ba/F3)	Parental (Ba/F3)
19a		9.0	56	3.6	26	1567
20a		19	162	4.4	14	2015
20b		18	250	3.4	42	890
20c		6.9	106	3.9	31	1857
20d		42	112	3.0	17	369
20e		69	639	10	500	1501
20f		2.3	9.0	0.9	13	1287
20g		8.6	40	1.2	8.8	1219

[a] All data in this study were obtained from in-house assays. In a different enzymatic assay conducted by Reaction Biology Corporation,[43] the IC$_{50}$s of **20g** were determined to be 0.37 nM (ABL) and 2.0 nM (ABL^{T315I}), as previously reported.[20]
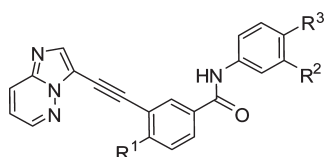
12b retained potency but also exhibited undesirable rat PK. Further attempts to cap the primary amine with the more stable cyclopropyl group which had previously led to the orally bioavailable compound **1a**,[21a] turned out to be unsuccessful. At this point, we recognized the need to determine whether the poor PK derived from C^8 substitution or the newly installed Ar−C≡C−Ar system itself. Previous experience with similar series (e.g., 9-[(aren)ethynyl]purines) suggested that inhibitors bearing free amino or acetamido moieties at the position equivalent to C^8 of the current template often exhibited undesirable PK. Thus, analogue **12c**, devoid of any C^8 substitution, was prepared and evaluated (Figure 3). Gratifyingly, this compound demonstrated good in vitro activity (Table 2) with excellent oral exposure (AUC$_{0-24 h}$/dose = 5476 ng*h/mL/mg/kg) and good oral bioavailability (42%) when tested in rats (Table 7). Furthermore, the cellular potency of **12c** and two other C^8-unsubstituted analogues **12d−e** correlated well with kinase activity, whereas inhibitors **12a** and **12b** exhibited larger disparities between both assays. Therefore, on the basis of the overall improved properties exhibited by **12c**, further SAR efforts focused on the C^8-unsubstituted 3-(arylacetylenyl)imidazo[1,2-*a*]pyridine chemical series.

Inhibitor Series Evolution. Despite a favorable PK profile, **12c** exhibited lower cellular potency against ABL^{T315I}, relative to **12a**. Attempts to increase potency through incorporation of water-soluble amines onto the imidazole ring resulted in only slightly increased cellular potency (**12d−e**, Table 2).

In further optimization, we sought to increase molecular recognition as a means to improve potency. To this end, inhibitor **19a** (Table 3), bearing a methylpiperazine moiety at C-4 on ring B, was designed. The terminal piperazinyl nitrogen atom was expected to be protonated at physiologic pH and the subsequent quaternary salt predicted to form an H-bond with the carbonyl oxygen atom of residue Ile360 in the activation loop of the protein (Figure 5). Such ligand−protein interactions have been previously observed in both imatinib:ABL (PDB: 1IEP) and bafetinib:ABL (PDB: 2E2B) crystal structures;[34,35] hence we expected the increased molecular interaction would enhance potency of the designed inhibitors against both native ABL and ABL^{T315I}. Moreover, piperazine is a widely utilized solubilizing group and its incorporation should improve cell permeability and help reduce lipophilicity and protein binding. Relative to **12c**, **19a** demonstrated 2-fold increased activity against the T315I mutated kinase and was approximately 20-fold more potent at inhibiting the growth of Ba/F3 cells expressing BCR-ABL^{T315I} (Table 3). Additionally, the presence of 340 μM human serum albumin minimally shifted the cellular potency of **19a** against native ABL (4 vs 5.9 nM) while a larger shift (8 to 51 nM) was observed with more lipophilic **12c**, suggesting that **19a** might exhibit less protein binding than **12c**. Finally, **19a** exhibited desirable pharmacokinetics when dosed orally in both rats and mice (Tables 7 and 8) and was subsequently identified as our first orally active BCR-ABL^{T315I} inhibitor in a pilot efficacy experiment (vide infra).
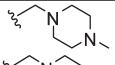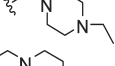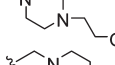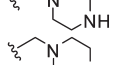
Table 5. SAR around Inhibitor **20g** (IC$_{50}$ in nM)
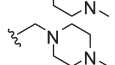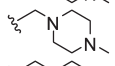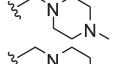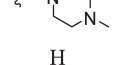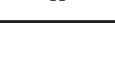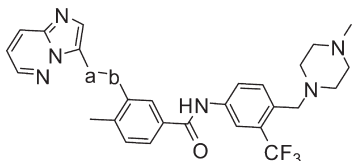
Cmpnd	R^1	R^2	R^3	ABL kinase	T315I kinase	ABL (Ba/F3)	T315I (Ba/F3)	Parental (Ba/F3)
20g	Me	CF$_3$		8.6	40	1.2	8.8	1219
20h	Me	CF$_3$		14	46	1.0	7.3	1158
20i	Me	CF$_3$		12	45	1.5	14	1684
20j	Me	CF$_3$		2.3	18	4.0	34	915
20k	H	CF$_3$		31	36	2.3	39	4213
20l	Cl	CF$_3$		41	95	2.5	8.6	1872
20m	F	CF$_3$		42	61	6.1	35	6289
20n	Me	Cl		2.4	82	2.3	210	1922
20o	Me	▷		5.3	71	3.9	256	1873
20p	Me	CF$_3$	H	19	988	10	1132	10000

Table 6. The Impact of Linker Hybridization on Potency (IC$_{50}$ in nM)

compd	a-b	ABL kinase	T315I kinase	ABL (Ba/F3)	T315I (Ba/F3)	parental (Ba/F3)
20g	C≡C	8.6	40	1.2	8.8	1219
24a	CH$_2$CH$_2$	19	317	4.3	295	5998
24b	*trans*-CH=CH	54	536	7.9	211	3241

Scheme 6. Synthesis of Aniline **17o**^{a}
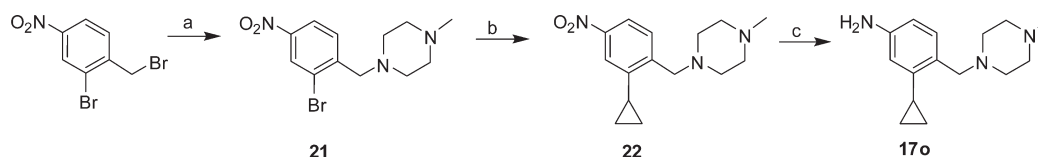
^{a} Reagents and conditions: (a) 1-methylpiperazine, Et$_3$N, CH$_2$Cl$_2$, rt; (b) cyclopropaneboronic acid, 10 mol % Pd(OAc)$_2$, 20 mol % P(c-hexyl)$_3$; K$_3$PO$_4$, Tol/H$_2$O, reflux; (c) Fe/HOAc, MeOH, reflux.

Encouraged by the overall properties of **19a**, further SAR around this series was explored. The reverse amide **19b** demonstrated similar potency, essentially preserving all elements of molecular recognition. Regioisomer **19c**, with the methylpiperazine *meta*, exhibited both decreased ABL^{T315I} kinase and cellular potency (5- and 10-fold, respectively) but was almost equipotent against native ABL. In our docking model, the terminal piperazinyl nitrogen in **19c** could also form an H-bond to the protein albeit with a different residue (Asp400), suggesting that the differential ABL^{T315I} activity observed between **19a** and **19c** may derive from increased van der Waals interactions of the piperazinyl ring on **19a** with

residues Val289, Phe359, and Asp381 in addition to the Ile360. SAR from other analogues further support this contention. The requirement of the piperazinyl H-bond was clearly demonstrated by the 12-fold decreased enzyme activity of the morpholine analogue **19d** against ABL^{T315I}. To the contrary, while the terminal nitrogens of *R*-3-(dimethylamino)pyrrolidinyl analogue **19e**, homopiperazinyl analogue **19f** and O-linked piperidinyl analogue **19g** were also predicted to form H-bonds with the protein; they all exhibited decreased potency relative to **19a**, supporting the optimal hydrophobic contact exhibited by the piperazinyl analogues. Attempts to further increase potency through terminal methyl group modifications (**19h−m**) were
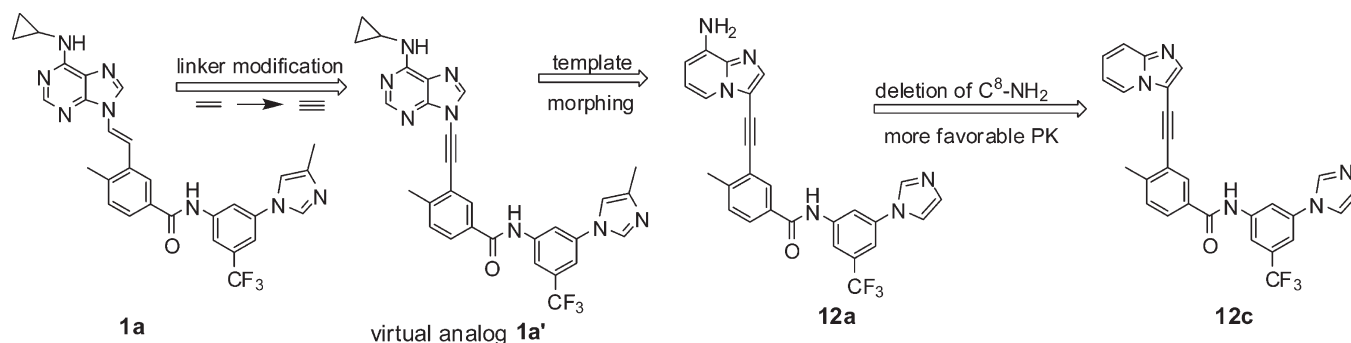
Figure 3. Generation of new lead **12c** based on multipoint variations of **1a**.

Scheme 7. Preparation of Inhibitor **24b**[a]
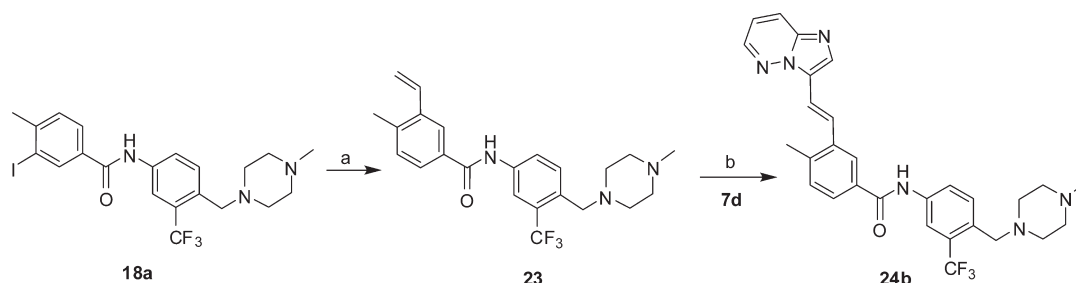
[a] Reagents and conditions: (a) 3 equiv tributyl(vinyl)tin, 2.7 mol % Pd$_2$(dba)$_3$, 20 mol % P(2-furyl)$_3$, DMF, rt; (b) 8 mol % Pd(OAc)$_2$, 16 mol % P(o-tol)$_3$, (i-Pr)$_2$NEt, DMF, 110 °C.

Figure 4. Model of **1a** (green) and its "virtual" acetylene-linked analogue **1a′** (cyan) bound to ABL^{T315I}.

unremarkable, with no compound offering any advantage relative to the parent inhibitor **19a**. Within this series (Table 3), potency against native ABL was insensitive to small inhibitor structural modificati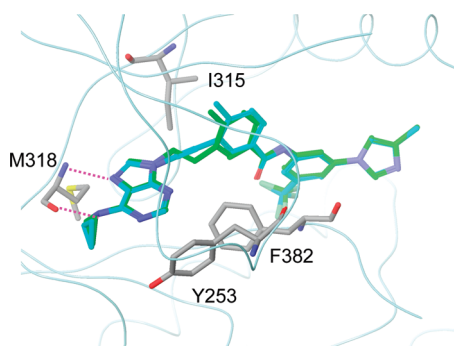ons, with most compounds exhibiting activity within a narrow range relative to ABL^{T315I} inhibition where much greater sensitivity to minor structural perturbations was observed.

Earlier success (Tables 2 and 3) with template morphing from purine to imidazo[1,2-a]pyridine encouraged us to next explore alternate heterocycles as hinge region binders. One approach focused on templates that could potentially form paired H-bonds with the protein; previously we had shown that an exocyclic NH at C-8 on the imidazo[1,2-a]pyridine core significantly increased potency (**12a** vs **12c**, Table 2). Because of the poor PK exhibited by this analogue (vide supra) and insights from other internal programs, we targeted inhibitors possessing endocyclic NHs as H-bond donors. Several diverse heterocyclic templates were selected for investigation (**20a–d**, Table 4), however, these inhibitors did not exhibit the expected potency improvement over **19a**. In general, ABL^{T315I} kinase

activity was reduced by 2−4-fold although two compounds (**20a** and **20d**) demonstrated slightly increased cellular potency. Simultaneously, we explored additional 6/5 fused aromatic ring systems and established a goal to reduce the lipophilicity of **19a** (clogP = 6.69)[36] through nitrogen atom incorporation. Three pyridine ring permutations with CH replaced by nitrogen were explored (each reduced the clogP by approximately 1 log unit). Inhibitor **20e**, with N occupying the H-bond donor C-8 position, markedly reduced potency. However, both **20f** and **20g** demonstrated increased enzyme and cellular potency relative to **19a**. Compound **20g** exhibited more favorable preliminary PK than **20f** (Table 7) and so its SAR was further explored.

SAR around 20g. To further explore SAR around the advanced lead compound **20g**, we re-examined distal piperazine nitrogen substitution and found that the SAR trends disclosed in Table 3 were largely preserved with this new template (Table 5). For example, **20h** and **20i**, both with larger N-substituents exhibited similar potency to **20g**. Not surprisingly, deletion of the entire methylpiperazinyl moiety (**20p**) markedly reduced ABL^{T315I} activity, with a decrease in potency of 25- and 130-fold in enzymatic and cellular assays, respectively. Next, the potency impact of the A-ring "flag-methyl"[37] group was briefly investigated. Chlorine substitution (**20l**) was essentially equipotent in inhibiting proliferation of BCR-ABL^{T315I} expressing Ba/F3 cells, whereas hydrogen or fluorine substitution (**20k**, **20m**) resulted in 3−4-fold potency loss. Last, B-ring trifluoromethyl replacement with either chlorine (**20n**) or cyclopropyl (**20o**) groups significantly reduced cellular potency against mutant T315I but only marginally affected activity against native ABL.

To confirm the absolute requirement of the carbon−carbon triple bond for the ABL^{T315I} potency of **20g**, we systematically added hydrogen back across this linker. As shown in Table 6, both the double bond linked and fully saturated molecules (**24a** and **24b**) significantly reduced ABL^{T315I} activity.

Table 7. Mean Pharmacokinetic Parameters Following Intravenous (iv) or Oral (po) Dosing in CD Rats[a]

	iv[b]			po[c]				
compd	CL (L/h/kg)	V_d (L/kg)	$t_{1/2}$ (h)	DN $AUC_{0-24\,h}$[d] (ng·h/mL/mg/kg)	C_{max} (ng/mL)	t_{max} (h)	$t_{1/2}$ (h)	F (%)
12a	0.36	8.2	15.8	151.9	234.3	1.0	5.2	5.5
12c	0.08	1.0	9.1	5745.9	2346.4	6.0	21.6	42.4
19a	0.75	11.0	10.2	386.3	148.7	6.0	24.7	29.0
20a	1.25	19.6	10.9	119	71	6.0	14.3	15
20b	2.04	15.9	5.4	BQL[e]	32.7	6.0		
20c	2.44	17.7	5.0	BQL	BQL			
20f	2.90	14.7	3.5	57.0	57.8	4.0	5.0	16.7
20g	0.65	9.7	10.2	278.5	204.8	6.0	11.0	18.2
20h	1.02	13.1	8.9	518.0	214.8	6.0	22.3	53.0
20i	1.53	7.7	3.5	145.3	164.1	4.0	3.4	22.3
20l	1.18	16.7	9.9	673.8	302.1	6.0	20.2	79.2
20m	0.37	3.1	5.9	1707.5	1184.7	6.0	11.6	62.3

[a] n = 3 animals per study. [b] Dosed at 5 mg/kg. [c] Dosed at 15 mg/kg. [d] DN AUC = AUC/dose. [e] BQL = below quantitation limit.
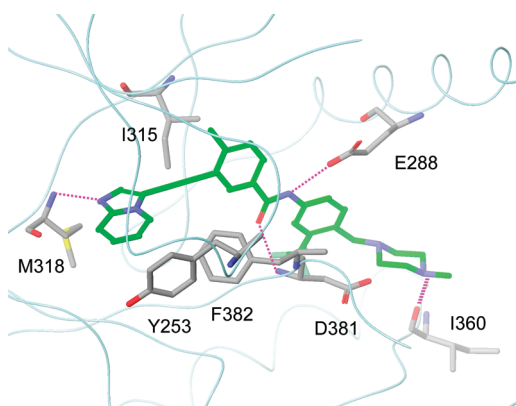
Figure 5. Model of inhibitor **19a** bound to ABL[T315I].

Table 8. Mouse PK Parameters Following Oral Dosing[a]

compd	dose (mg/kg)	$AUC_{0-24\,h}$ (ng·h/mL)	C_{max} (ng/mL)	$t_{1/2}$ (h)
19a	30	11253	985.9	2.9
20f	30	2694	521.4	2.7
20i	30	13710	1327.2	2.4
20l	30	6075	441.1	2.9
20g	30	4713	416.3	2.9
20g	10	2086	209.9	3.2
20g	5	995	122.7	3.2

[a] n=3 animals per study. **20h** and **20m** were evaluated in an abbreviated assay in which plasma concentrations at 2, 6, and 24 h were determined and the following results were obtained: for **20h**, these concentrations were 622.5, 387.4, and 8.8 ng/mL, respectively, when dosed at 30 mg/kg; for **20m**, 2475.8, 2098.7, and 163.1 ng/mL. For comparison, **20g** demonstrated concentrations of 416.3, 298.9, and 4.2 ng/mL.
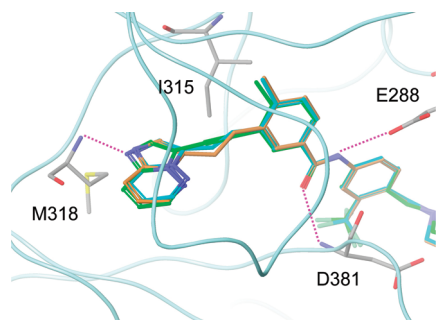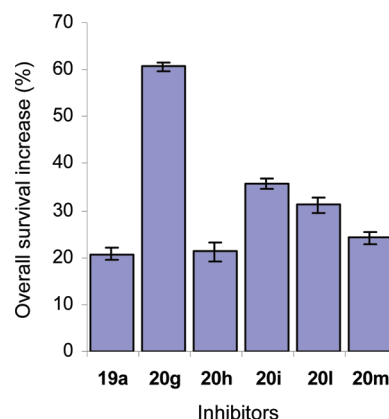

Figure 6. X-ray structure of ABL[T315I] in complex with inhibitor **20g** (green) and model of **24a** (brown) and **24b** (cyan).

Figure 7. In vivo efficacy of inhibitors in a Ba/F3 BCR-ABL[T315I] survival model at dose level of 10 mg/kg (error bars represent SD).

Elsewhere, we have reported the three-dimensional structure of the ABL[T315I]:**20g** complex (PDB: 3IK3).[20] The crystal structure confirmed that **20g** binds to the DFG-out conformation of the protein (Figure 6), and the key molecular recognition components are consistent with those predicted by modeling shown in Figures 4 and 5. The coordinates from this crystal structure were used to refine the docking model for alternate linker analogues **24a** and **24b** (Table 6), and the inhibitor–protein interactions were compared. All three analogues bind to the protein in a similar fashion, and all three linkers can evade steric clash from the bulky gatekeeper isoleucine. One explanation for their differing potencies is that the least sterically demanding acetylene linker makes more favorable van der Waals' contact with gatekeeper Ile315 and Phe382 of the DFG motif (the triple bond is 3.4–3.6 Å away from Ile315 and also almost bisected by the aromatic ring of Phe382 in the crystal structure). Another potential factor contributing to the high ABL[T135I] potency of **20g** is that the rigidity of the acetylene linkage promotes an extended conformation of the unbound inhibitor, which favors binding to ABL[T315I] in a DFG-out mode. The more flexible linkers in **24a** and **24b** could bring about a folded conformation in the unbound inhibitors; transition to an extended conformation would be entropically less favorable and hence reduce potency.

Taken together, the SAR studies on **20g** show that, as with the preceding chemical series, the gatekeeper T315I mutant is a more "stringent" target than native ABL. Minor structural modifications to either the acetylene linker,
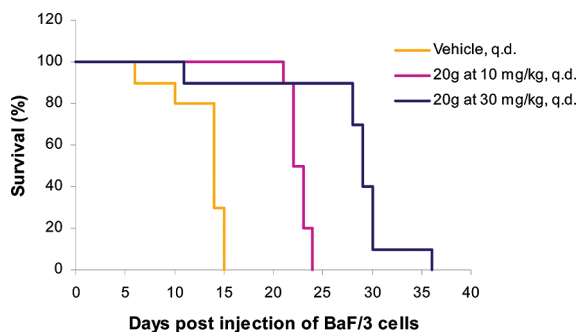
Figure 8. In vivo efficacy of **20g** in a Ba/F3 BCR-ABL[T315I] survival model.

the methylpiperazinyl moiety, or the trifluoromethyl group significantly affected ABL[T315I] potency while modifications or even deletion of one of these binding elements still yielded potent native ABL inhibitors. We conclude that incorporation of multiple points of protein contact led to the high potency of **20g** against the refractory ABL mutant T315I.

Pharmacokinetics. During this program, potent inhibitors were continually evaluated for their pharmacokinetic (PK) properties in rats immediately following assessment of their in vitro activity (Table 7). In general, inhibitors bearing imidazole as the B ring appendage demonstrated higher dose normalized AUC and C_{max} than those piperazine-containing compounds (**12c** vs **19a**). **12c** had a much smaller volume of distribution relative to **19a**, consistent with a highly protein bound species, which was confirmed by a potency shift in vitro in the presence of human serum albumin (vide supra). The exocyclic NH_2 at C-8 on the imidazo[1,2-*a*]pyridine template drastically reduced both AUC and C_{max} of imidazole-bearing inhibitors to the level of piperazine-containing compounds (**12c** vs **12a** and **19a**).

Among those piperazine-bearing inhibitors possessing alternate hinge binding templates, **20b** and **20c** exhibited low oral absorption in rats. For the remaining inhibitors, their dose normalized oral exposure in rats were ranked as follows: **19a** > **20g** > **20a** ≫ **20f**, and C_{max} **20g** > **19a** ≫ **20a** ≈ **20f**. Both **20g** and **19a** exhibited long half-lives and reduced clearance relative to **20f**. The latter exhibited the highest clearance and hence lowest AUC. Five inhibitors (**20g**, **20h**, **20i**, **20l**, **20m**) bearing the same template, imidazo[1,2-*b*]-pyridazine in general demonstrated good PK.

Mouse PK data for these inhibitors were collected as a prerequisite to evaluating potency in in vivo efficacy models (Table 8). In general, mouse PK exhibited similar trends to those observed in rats. For **20g**, PK parameters were determined orally at different doses; good dose proportionality was observed.

The concentration of **20g** in the brain was also measured to evaluate its ability to penetrate the blood−brain barrier (BBB). In a mouse PK study following a single oral 30 mg/kg dose, a brain/plasma concentration ratio of 1.60 was determined at 6 h postdosing, indicating high levels of BBB penetration. It should be noted that among the three approved agents for CML treatment, only dasatinib crosses the blood−brain barrier, with human cerebrospinal fluid/plasma ratios ranging from 0.05 to 0.28.[38] Among the inhibitors in clinical trials, bafetinib demonstrated 10-fold lower brain levels compared to plasma in mice. Despite the low levels, this concentration is sufficient for bafetinib to inhibit the growth of Ph+ leukemic cells in the murine CNS.[39] The higher level of BBB penetration for **20g**

might suggest it has greater potential in treating CNS Ph+ leukemia that often complicates late-stage CML.

In Vivo Efficacy. Several inhibitors possessing desirable in vitro kinase and cellular potency and with favorable pharmacokinetic profiles were evaluated for their antitumor activity in an aggressive mouse model of CML driven by the T315I mutation. In this model, Ba/F3 cells expressing BCR-ABL[T315I] were injected into the tail vein of SCID mice. After 3 days, the animals were dosed orally with inhibitors at 10 mg/kg, once daily for 19 consecutive days. The level of increased overall survival of treated mice relative to untreated control was used to assess efficacy. Median survival of untreated mice in this model was 14 days. Among all six inhibitors tested, **20g** demonstrated the greatest increased overall survival (Figure 7). At the higher dose of 30 mg/kg/day, **20g** more than doubled the survival of animals in this highly aggressive model (Figure 8) and was well tolerated for the duration of study with no signs of overt toxicity.

Kinase and Mutant Selectivity Profile of 20g. To assess the kinase selectivity profile of **20g** beyond ABL, broad panel kinase screening was conducted using an enzymatic assay as previously reported.[20] In brief, **20g** was found to be a multi-targeted inhibitor with activity against FLT3, FGFR, and VEGFR family kinases in the single digit nanomolar range. Like imatinib, nilotinib, and dasatinib, **20g** also inhibits c-Kit and PDGFRα/β. Many of these kinases are important clinical targets in a variety of other malignancies and support the potential testing of **20g** more broadly against a range of cancers. To the contrary, **20g** does not inhibit Aurora kinases and demonstrated over 500-fold selectivity relative to a number of kinases including CDK2/cyclin E, EGFR, FAK, IGF1R, JAK2, and c-Met. The relatively broad kinase specificity profile of **20g** can likely be attributed to the linear ethynyl linkage, which permits binding to kinases with hydrophobic residues at the gatekeeper position.

Elsewhere, we have reported the cellular activity of **20g** against a broad panel of clinically relevant BCR-ABL mutants, confirming its pan-BCR-ABL activity.[20] Briefly, **20g** was active against all tested mutants including, but not limited to, T315A, F317L/V, Y253H, E255K/V, and F359V, mutations which have been reported in patients failing on either dasatinib or nilotinib.[11,12,40] Additionally, in an accelerated mutagenesis screen for resistance, **20g** completely suppressed the outgrowth of all mutants at a concentration of 40 nM. Together, these results are consistent with the profile of a true pan-BCR-ABL inhibitor, active against the native enzyme and all clinically relevant mutants including T315I.

Conclusion

Starting from **1a**, a lead compound that emerged from our program developing DFG-out targeted ABL kinase inhibitors based on the 9-[(aren)ethenyl]purine template, extensive medicinal chemistry coupled with detailed structural investigations has led to a novel series of kinase inhibitors that potently inhibit native ABL and a broad panel of clinically relevant mutants including T315I at the gatekeeper position (Figure 2). Crystallographic studies confirmed that this series binds to the inactive, "DFG-out" conformation of the protein. One unusual structural feature of these potent inhibitors is the inflexible acetylene linkage connecting the heterocycle core serving as the hinge binder and the *N*-arylbenzamide occupying the hydrophobic selectivity pocket.[41] This rigid, less sterically demanding linker enables binding to the enlarged Ile315 side chain of the T315I mutant and correctly directs both inhibitor segments into well-defined

binding pockets making more productive interactions with the protein. Another key structural element required for achieving high potency is the hybrid *N*-arylbenzamide, which allows cooperative molecular exploitation of both trifluoromethyl and piperazinyl groups to maximize van der Waals and hydrogen-bonding interactions with the protein. In general, the piperazine tail confers excellent cellular potency and improved aqueous solubility with reduced plasma protein binding, leading to favorable pharmacokinetic properties following oral dosing in rats and mice. Inhibitor **20g** exhibited low nM cellular potency against cells lines expressing either native BCR-ABL or BCR-ABL[T315I] and significantly prolonged survival in an aggressive mouse model of CML driven by the T315I mutant. **20g** also potently inhibited proliferation of all clinically relevant ABL mutants in cell-based assays characterizing it as the first pan-BCR-ABL inhibitor. On the basis of these data, and its favorable overall ADME profile, **20g** was nominated as a development candidate and is currently undergoing phase I clinical evaluation in patients with refractory CML and other hematologic malignancies.[42]

Experimental Section

General Chemistry. All reagents and solvents were used as received. ^{1}H NMR spectra were recorded on a Bruker ARX300 or a Bruker AVANCE400 spectrometer using TMS as internal standard. MS spectra were recorded on a Waters Micromass ZQ spectrometer. Elemental analyses were performed by Robertson Microlit Laboratories in Madison, NJ. HPLC was performed on an Agilent 1100 HPLC system. The purity of all SAR compounds was determined to be ≥95% by reverse phase HPLC (C-18 column, MeCN/H_2O with 0.1% CF_3CO_2H as the mobile phase).

Cyclopropyl-(9-trichlorovinyl-9*H*-purin-6-yl)amine (3). A solution of 6-(cyclopropylamino)-9*H*-purine (3 g, 17.1 mmol) in anhydrous HMPA (156 mL) was added to NaH (1.5 g, 60% dispersion in oil) under stirring until no effervescence was observed. Tetrachloroethylene was then added dropwise, and the mixture was heated at 60 °C overnight. Excess HMPA was distilled off, and the resultant mixture was quenched with methanol. The crude was extracted with EtOAc, washed with water, and then dried over Na_2SO_4. The solvent was removed, and the resultant residue was chromatographed over silica gel eluting with hexanes−EtOAc to furnish the desired product (0.65 g, 12% yield). ^{1}H NMR (CDCl$_3$): δ 0.60 (m, 2H), 0.81 (m, 2H), 3.10 (m, 1H), 6.60 (br, 1H), 7.80 (s, 1H), 8.50 (s, 1H).

Cyclopropyl-(9-ethynyl-9*H*-purin-6-yl)amine (4). To the solution of **3** (0.5 g, 1.65 mmol) in THF (17 mL) was added *n*-BuLi (2.6 mL, 6.56 mmol) at −78 °C. The reaction mixture was stirred at this temperature for one additional hour and then carefully quenched with methanol. The solvent was stripped off, and the resultant residue was partitioned between EtOAc and water. After drying and concentration, the crude was chromatographed over silica gel eluting with hexanes−EtOAc (6:4) to furnish the desired product (0.1 g, 30% yield). ^{1}H NMR (CDCl$_3$): δ 0.50 (m, 2H), 0.72 (m, 2H), 2.80 (m, 1H), 3.10 (s, 1H), 5.90 (s,1H), 7.80 (s, 1H), 8.30 (s, 1H). MS: *m/z* 200.0 [M + H]$^+$.

N*-{3-[2-[(Dimethylamino)methyl]-1*H*-imidazol-1-yl]-5-(trifluoromethyl)phenyl}-3-iodo-4-methylbenzamide (5d). This was prepared analogously to **5c** via a published procedure[25] using **14**[44] instead of imidazole. ^{1}H NMR (CDCl$_3$): δ 2.21 (s, 9H), 3.30 (s, 2H), 7.10 (s, 2H), 7.55 (m, 4H), 7.65 (s, 2H). MS: *m/ztalic > 529.0* [*M* + H]$^+$.

3-{2-[6-(Cyclopropylamino)purin-9-yl]ethynyl}-4-methyl-*N*-[4-(trifluoromethyl)-pyridin-2-yl]-benzamide (6a). Iodobenzamide **5a**[21a] (0.44 g, 1.1 mmol) and alkyne **4** (0.2 g, 1.0 mmol) was dissolved in a mixture of toluene and triethylamine (10 mL, 1:2). To this was added Pd(PPh$_3$)$_4$ (0.062 g, 0.05 mmol) and CuI (0.0051 g, 0.026 mmol). The resulting solution was degassed by a stream of argon for 30 min and then heated at 55 °C for 3 h. The crude was chromatographed over silica gel eluting with hexanes−EtOAc (2:8) to furnish a pale-yellow solid, which was further washed with cold methanol to afford pure product (0.029 g, 6% yield). ^{1}H NMR (CDCl$_3$): δ 0.50 (m, 2H), 0.62 (m, 2H), 2.31 (s, 3H), 2.80 (s, 1H), 5.90 (s, 1H), 7.25 (m, 1H), 7.40 (d, *J* = 8.0 Hz, 1H), 7.70 (d *J* = 2 Hz, 1H), 7.80 (s, 1H), 8.05 (d, *J* = 1.9 Hz, 1H), 8.40 (d, *J* = 5.1 Hz, 1H), 8.50 (s, 1H), 8.61 (s, 1H), 8.65 (s, 1H). MS: *m/z* 479.1 [M + H]$^+$.

3-{2-[6-(Cyclopropylamino)purin-9-yl]ethynyl}-*N*-[5-(1,1-dimethylethyl)isoxazol-3-yl]-4-methylbenzamide (6b). This was prepared analogously to **6a** using **5b**[21a] and **4**. ^{1}H NMR (CDCl$_3$): 0.80 δ (m, 2H), 1.00 (m, 2H), 1.70 (s, 9H), 2.61 (s, 3H), 3.10 (s, 1H), 6.50 (s, 1H), 7.05 (s, 1H), 7.60 (d, *J* = 8.0 Hz, 1H), 8.00 (d, *J* = 2.0 Hz, 1H), 8.11 (s, 1H), 8.25 (d, *J* = 1.8 Hz, 1H), 8.70 (s, 1H), 9.25 (s, 1H). MS: *m/z* 457.0 [M + H]$^+$.

3-Bromoimidazo[1,2-*a*]pyridin-8-ylamine (7a). To a solution of **7b** (10.24 g, 40.30 mmol) in EtOH (500 mL) was added concentrared aq HCl (51 mL). The suspension was refluxed for 2 h. Upon cooling, the reaction mixture was basified under stirring with 10 N NaOH until the pH reached ~9. EtOH was removed on a rotavap and the resulting suspension was partitioned in CH_2Cl_2 and H_2O. The organic layer was dried and concentrated, giving the desried product as a brownish solid (7.66 g, 90%). ^{1}H NMR (DMSO-*d$_6$*): δ 5.79 (br, 2H), 6.36 (d, *J* = 7.4 Hz, 1H), 6.84 (dd, *J* = 6.9, 7.2 Hz, 1H), 7.57 (s, 1H), 7.62 (d, *J* = 7.4 Hz, 1H).

N*-(3-Bromoimidazo[1,2-*a*]pyridin-8-yl)acetamide (7b). Bromine was added dropwise to a solution of 8-acetamidoimidazo-[1,2-*a*]pyridine[24] (8.0 g, 45.7 mmol) in EtOH at 0 °C. The solution was stirred at rt for 3 h, at which point HPLC indicated complete conversion. After the volatile components were removed on a rotavap, the residue was taken up in CH_2Cl_2 and then washed with saturated aq NaHSO$_3$ and then 1N NaOH until the pH reached 7. The organic layer was passed through celite, dried over Na_2SO_4, and concentrated on a rotavap, giving essentially pure material by NMR and HPLC. ^{1}H NMR (DMSO-*d$_6$*): δ 2.22 (s, 3H), 7.06 (dd, *J* = 7.2, 7.3 Hz, 1H), 7.74 (s, 1H), 8.05−8.08 (m, 2H), 10.06 (s, 1H).

N*-(3-Bromoimidazo[1,2-*a*]pyridin-8-yl)imidodicarbonic Acid, *C,C*′-Bis(1,1-dimethylethyl)ester (7a′). To a solution of **7a** (5.75 g, 27.12 mmol) in THF (120 mL) was added Boc$_2$O (3 equiv) and DMAP (0.1 equiv). After the mixture was stirred at rt for 18 h, the solvent was removed and the residue was suspended in EtOAc. Filtration gave a brownish solid, which was determined by NMR to be pure product. The filtrate was concentrated and purified by CombiFlash chromatography (30% EtOAc in hexanes), giving the second crop of product. The combined yield was 78%. ^{1}H NMR (DMSO-*d$_6$*): δ 1.38 (s, 18H), 7.15 (dd, *J* = 7.0, 7.3 Hz, 1H), 7.39 (d, *J* = 7.3 Hz, 1H), 7.82 (s, 1H), 8.39 (d, *J* = 7.3 Hz, 1H).

General Procedure for the Preparation of Arylacetylenes 9: 3-ethynylimidazo[1,2-*a*]pyridine (9c). To a solution of **7c** (5 g, 25.4 mmol) in MeCN (50 mL) was added Pd(PPh$_3$)$_2$Cl$_2$ (0.445 g, 0.634 mmol), CuI (0.17 g, 0.89 mmol), dicyclohexylamine (5.6 mL, 28 mmol), and ethynyltrimethylsilane (7.2 mL, 51 mmol). The solution was purged with argon for 15 min, sealed, and heated at 80 °C for 3 h, at which point HPLC indicated disappearance of starting bromide. The solvents were concentrated and to the residue was added H_2O and CH_2Cl_2 (25 mL each). The organic layer was separated, and the aqueous layer was repeatedly extracted with CH_2Cl_2 (3 × 20 mL). The combined extracts were dried (Na$_2$SO$_4$) and concentrated (R_f = 0.47 in 50% hexanes in EtOAc). The resulting residue was dissolved in THF (100 mL) and treated with tetrabutyl ammonium fluoride monohydrate (8.3 g, 32 mmol) in H_2O (5 mL), and the mixture was stirred at rt for 2 h. The solvents were concentrated, and the resulting residue was partitioned between H_2O (25 mL) and CH_2Cl_2 (150 mL). The aqueous layer was extracted with CH_2Cl_2 (2 × 30 mL). The combined extracts were dried over Na_2SO_4 and concentrated on

a rotavap. The resulting residue was purified by combiflash on silica gel using hexanes−EtOAc. The desired product was eluted with 50% hexanes in EtOAc and isolated as an off-white solid in 84% yield. ^{1}H NMR (DMSO-d_6): δ 5.08 (s, 1H), 7.13 (ddd, J = 0.9, 6.8, 6.9 Hz, 1H), 7.42 (ddd, J = 1.2, 6.8, 6.9 Hz, 1H), 7.71 (d, J = 6.9 Hz, 1H), 7.96 (s, 1H), 8.46 (d, J = 6.8 Hz, 1H). MS: m/z 200 [M + H]$^+$.

N-(3-Ethynylimidazo[1,2-a]pyridin-8-yl)imidodicarbonic Acid, C,C′-Bis(1,1-dimethylethyl)ester (9a). This was made from **7a** via bis-Boc protection. ^{1}H NMR (DMSO-d_6): δ 1.34 (s, 18H), 5.11 (s, 1H), 7.13 (dd, J = 6.8, 7.3 Hz, 1H), 7.39 (dd, J = 0.9, 7.3 Hz, 1H), 7.95 (s, 1H), 8.46 (dd, J = 0.9, 6.8 Hz, 1H).

N-(3-Ethynylimidazo[1,2-a]pyridin-8-yl)acetamide (9b). ^{1}H NMR (DMSO-d_6): δ 2.23 (s, 3H), 5.08 (s, 1H), 7.06 (dd, J = 6.9, 7.4 Hz, 1H), 7.94 (s, 1H), 8.11 (d, J = 7.6 Hz, 1H), 8.16 (dd, J = 0.9, 6.7 Hz, 1H), 10.10 (s, 1H).

3-Ethynylimidazo[1,2-b]pyridazine (9d). ^{1}H NMR (DMSO-d_6): δ 4.93 (s, 1H), 7.35 (dd, J = 4.4, 9.2 Hz, 1H), 8.11 (s, 1H), 8.21 (dd, J = 1.6, 9.2 Hz, 1H), 8.65 (dd, J = 1.6, 4.4 Hz, 1H).

General Procedure for the Preparation of Inhibitors 12: 3-[2-(8-Aminoimidazo[1,2-a]pyridin-3-yl)ethynyl]-N-[3-(1H-imidazol-1-yl)-5-(trifluoromethyl)phenyl]-4-methylbenzamide (12a). Alkyne **9a** (130 mol %), iodobenzamide **5c** (0.2 mmol), Pd[(PPh$_3$)$_4$] (5 mol %), and CuI (7.5 mmol %) was placed in a vial with rubber septum. The mixture underwent 3 cycles of vacuum/filling with N$_2$. DMF (1.5 mL) and N,N-diisopropylethylamine (150 mol %) was then added. The mixture was stirred at rt for 16 h and then quenched with H$_2$O. EtOAc and more water were added for extraction. The combined organic layer was dried (over Na$_2$SO$_4$), filtered, concentrated, and the resulting residue was purified by silica gel chromatography (eluent: 5% MeOH in CH$_2$Cl$_2$), giving the **12a′** as an off-white solid. Standard deprotection to cleave both Boc groups with TFA furnished **12a**. ^{1}H NMR (DMSO-d_6): δ 2.74 (s, 3H), 5.85 (br, 2H), 6.60 (d, J = 7.4 Hz, 1H), 7.06 (dd, J = 7.0, 7.1 Hz, 1H), 7.42 (s, 1H), 7.69 (d, J = 8.1 Hz, 1H), 7.86−8.10 (m, 5H), 8.38 (s, 1H), 8.40 (d, J = 1.3 Hz, 1H), 8.52 (s, 1H), 8.65 (s, 1H), 10.92 (s, 1H). MS: m/z 500.9 [M + H]$^+$.

3-{2-[8-(Acetylamino)imidazo-[1,2-a]pyridin-3-yl]ethynyl}-N-[3-(1H-imidazol-1-yl)-5-(trifluoromethyl)phenyl]-4-methylbenza-mide (12b). This was made from coupling of **9b** and **5c**. ^{1}H NMR (DMSO-d_6): δ 2.10 (s, 3H), 2.70 (s, 3H), 7.22 (dd, J = 6.6, 7.4 Hz, 1H), 7.92 (d, J = 7.9 Hz, 1H), 7.71−8.47 (m, 11H), 10.22 (s, 1H), 10.83 (s, 1H). MS: m/z 542.9 [M + H]$^+$.

N-[3-(1H-Imidazol-1-yl)-5-(trifluoromethyl)phenyl]-3-[2-(imidazo-[1,2-a]pyridin-3-yl)ethynyl]-4-methylbenzamide (12c). This was made from coupling of **9c** and **5c**. ^{1}H NMR (DMSO-d_6): δ 2.64 (s, 3H), 7.21 (dd, J = 6.6, 6.7 Hz, 1H), 7.68 (dd, J = 7.0, 7.1 Hz, 1H), 7.59 (d, J = 8.1 Hz, 1H), 7.72−7.88 (m, 3H), 7.97 (dd, J = 1.8, 8.0 Hz, 1H), 8.10 (s, 1H), 8.24 (s, 1H), 8.31 (dd, J = 1.7, 8.0 Hz, 1H), 8.36 (overlapped singlet, 2H), 8.64 (d, J = 6.6 Hz, 1H), 10.76 (s, 1H). MS: m/z 486.0 [M + H]$^+$.

N-{3-[2-[(Dimethylamino)methyl]-1H-imidazol-1-yl]-5-(trifluoromethyl)phenyl}-3-[2-(imidazo[1,2-a]pyridin-3-yl)ethynyl]-4-methylbenzamide (12d). This was made from coupling of **9c** and **5d** in 59% yield. ^{1}H NMR (CDCl$_3$): δ 2.41 (s, 6H), 2.50 (s, 3H), 3.75 (s, 2H), 6.90 (m, 1H), 7.00 (s, 1H), 7.11 (s, 1H), 7.30 (d, J = 6.1 Hz, 2H), 7.60 (m, 1H), 7.71 (s, 1H), 7.83 (m, 1H), 8.11 (s, 2H), 8.33 (m, 3H), 9.60 (s, 1H). MS: m/z 543.9 [M + H]$^+$.

3-[2-(Imidazo[1,2-a]pyridin-3-yl)ethynyl]-4-methyl-N-{3-[4-(1-pyrrolidinylmethyl)-1H-imidazol-1-yl]-5-(trifluoromethyl)phenyl}-benzamide (12e). This was made analogously to **12d** using pyrrolidine instead of dimethylamine in the first step of the reaction sequence depicted in Scheme 3. ^{1}H NMR (DMSO-d_6): δ 2.20 (m, 4H), 2.51 (s, 3H), 3.55 (m, 6H), 7.40 (m, 1H), 7.70 (m, 1H), 7.83 (d, J = 8.2 Hz, 1H), 8.0 (d, J = 8.5 Hz, 1H), 8.11 (s, 1H), 8.20 (m, 2H), 8.30 (s, 1H), 8.44 (s, H), 8.50 (d, J = 1.6 Hz, 1H), 8.74 (m, 2H), 8.90 (d, J = 6.6 Hz, 1H), 11.1 (s, 1H). MS: m/z 568.9 [M + H]$^+$.

1-Methyl-4-{[4-nitro-2-(trifluoromethyl)phenyl]methyl}pipe-razine (16a). A suspension of 2-methyl-5-nitrobenzotrifluoride (3.90 g, 19 mmol), N-bromosuccinimide (NBS, 3.56 g, 20 mmol), and 2,2′-azobis(2-methylpropionitrile) (AIBN, 94 mg, 0.6 mmol)

in CCl$_4$ (40 mL) was refluxed under N$_2$ for 16 h, at which point HPLC indicated ca. 50% conversion. More NBS (10 mmol) and AIBN (0.6 mmol) was added, and the mixture was refluxed for another 14 h. HPLC indicated ca. 80% conversion. The reaction mixture was cooled down, and the solid was filtered off and washed with EtOAc. The combined filtrate was washed with aq NaHCO$_3$, dried over Na$_2$SO$_4$, filtered, concentrated on rotavap, and further dried under vacuum. ^{1}H NMR indicated the ratio of desired product 2-(bromomethyl)-5-nitrobenzotrifluoride to unreacted 2-methyl-5-nitrobenzotrifluoride was 75:25, based on the integration of CH$_2$Br (4.68 ppm in CDCl$_3$) and CH$_3$ (2.63 ppm). This material was not purified but used directly in the next step.

To a solution of crude 2-(bromomethyl)-5-nitrobenzotri-fluoride (13.33 mmol, 75% pure) in CH$_2$Cl$_2$ (10 mL) was added Et$_3$N (1.4 mL, 10 mmol) and 1-methylpiperazine (1.1 mL, 10 mmol). After stirring for 3 h at rt, aq NaHCO$_3$ was added, and the mixture was extracted with CH$_2$Cl$_2$. The combined organic layer was dried over Na$_2$SO$_4$, filtered, concentrated, and the resulting residue was purified by silica gel chromatography (eluent: 10% MeOH in CH$_2$Cl$_2$), giving the product as a pale-yellow oil (72%, 2.21 g). ^{1}H NMR (CDCl$_3$): δ 2.46 (s, 3H), 2.66 (m, 8H), 3.84 (s, 2H), 8.10 (d, J = 8.4 Hz, 1H), 8.32 (dd, J = 2.3, 8.4 Hz, 1H), 8.58 (d, J = 2.3 Hz, 1H).

4-[(4-Methylpiperazin-1-yl)methyl]-3-(trifluoromethyl)aniline (17a). A suspension of **16a** (1.23 g, 4 mmol) and sodium hydrosulfite (7.0 g, 85% pure from Aldrich, 40 mmol) in acetone and water (1:1, 20 mL) was refluxed for 3 h. Upon cooling, the volatile components (mainly acetone) were removed on rotavap, and the resulting mixture was subjected to filtration. The solid was thoroughly washed with EtOAc. The combined filtrate was extracted with n-BuOH (4×), and the combined organic layer was washed with saturated aq NaHCO$_3$, dried (Na$_2$SO$_4$), filtered, concentrated, and the resulting residue was purified by silica gel chromatography (eluent: 5% MeOH in CH$_2$Cl$_2$, MeOH was presaturated with ammonia gas), giving the product as a pale-yellow solid (65%, 0.71 g). ^{1}H NMR: (CDCl$_3$): δ 2.25 (s, 3H), 2.44 (m, 8H), 3.46 (s, 2H), 3.84 (br, 2H), 6.75 (dd, J = 2.3, 8.3 Hz, 1H), 6.88 (d, J = 2.4 Hz, 1H), 7.44 (d, J = 8.3 Hz, 1H).

3-Iodo-4-methyl-N-{4-[(4-methylpiperazin-1-yl)methyl]-3-(tri-fluoromethyl)phenyl}-benzamide (18a). 3-Iodo-4-methylbenzoyl chloride (0.48 g, 1.7 mmol), prepared from the reaction of 3-iodo-4-methylbenzoic acid and SOCl$_2$, was added to a solution of **17a** (0.47 g, 1.7 mmol), N,N-diisopropylethylamine (0.26 g, 2.0 mmol), and a catalytic amount of DMAP in THF (10 mL). After stirring at rt for 2 h, the reaction was quenched with water. EtOAc was added and the layers separated. The combined organic layers were concentrated to dryness and purified by silica gel chromatography (eluent: 5% MeOH in CH$_2$Cl$_2$, MeOH was presaturated with ammonia gas), giving the desired product as an off-white solid (57%, 0.51 g). ^{1}H NMR: (acetone-d_6): δ 2.07 (s, 3H), 2.26 (m, 8H), 2.37 (s, 3H), 3.50 (s, 2H), 7.36 (d, J = 7.9 Hz, 1H), 7.67 (d, J = 8.5 Hz, 1H), 7.84 (dd, J = 1.8, 8.5 Hz, 1H), 7.92 (dd, J = 1.9, 8.5 Hz, 1H), 8.11 (d, J = 2.2 Hz, 1H), 8.33 (d, J = 1.8 Hz, 1H), 9.66 (s, 1H).

N-(3-Iodo-4-methylphenyl)-4-[(4-methyl-1-piperazinyl)methyl]-3-(trifluoromethyl)-benzamide (18b). N-(4-(4-Methylpiperazin-1-yl)methyl)-3-(trifluoromethyl benzoic acid[26] (1.0 g, 2.67 mmol) and 3-iodo-4-methyl aniline (0.68 g, 2.90 mmol) were dissolved in DMF (14 mL). To this, HATU (1.5 g, 4.00 mmol) and DIPEA (1.5 mL) were added and the mixture was stirred overnight. The solvent was removed under vacuum, and the crude residue was chromatographed over silica gel eluting initially with EtOAc and then with CH$_2$Cl$_2$−MeOH (95:5), giving the desired product (0.98 g, 70%). ^{1}H NMR (CDCl$_3$): δ 2.20 (s, 3H), 2.21 (s, 3H), 2.50 (m, 8H), 3.76 (s, 2H), 7.15 (d, J = 8.2 Hz, 1H), 7.50 (m, 1H), 7.73 (br, 1H), 7.90 (s, 2H), 8.00 (s, 2H). MS: m/z 518.0 [M + H]$^+$.

3-Iodo-4-methyl-N-[4-(1-methylpiperidin-4-yloxy)-3-(trifluoro-methyl)phenyl]benz-amide (18g). This was made from the reaction of 3-iodo-4-methylbenzoyl chloride with 4-(1-methylpiperi-din-4-yloxy)-3-(trifluoromethyl)aniline,[27] as described in the synthesis of **18a**. MS: m/z 518.9 [M + H]$^+$.

N-{4-[(4-(2-Fluoroethyl)piperazin-1-yl)methyl]-3-(trifluoromethyl)phenyl}-3-iodo-4-methylbenzamide (18k). Iodobenzamide **18l** was prepared analogously to **18a** using *N*-Boc-piperazine instead of *N*-methylpiperazine in the first step of the reaction sequence depicted in Scheme 4. **18l** (0.5 g) was then treated with TFA (10 mL) for 3 h. Excess solvent was removed, and the resultant salt was dissolved in DMF (4 mL). 2-Bromofluoroethane (0.15 mL) and NaHCO$_3$ (0.4 g) was then added, and the resulting mixture was heated at 80 °C for overnight. Solvent was evaporated; the residue was taken up in EtOAc and washed with water. The combined layer was dried over Na$_2$SO$_4$ and concentrated under vacuum. The residue was then flash chromatographed over silica gel eluting with CH$_2$Cl$_2$−MeOH (95:5) to furnish the desired product (0.25 g). ^{1}H NMR (CDCl$_3$): δ 2.41 (m, 4H), 2.51 (s, 3H), 2.50 (m, 6H), 3.82 (s, 2H), 4.50 (m, 1H), 4.69 (m, 1H), 7.25 (m, 1H), 7.80 (m, 5H), 8.20 (s, 1H). MS: *m/z* 518.9 [M + H]$^+$.

N-{3-Cyclopropyl-4-[(4-methylpiperazin-1-yl)methyl]phenyl}-3-iodo-4-methyl-benzamide (18o). To a solution of 2-bromo-4-nitrobenzyl bromide (1.56 g, 3.4 mmol) in CH$_2$Cl$_2$ (10 mL) was added Et$_3$N (0.48 mL, 3.4 mmol) and *N*-methylpiperazine (0.38 mL, 3.4 mmol) at 0 °C. The reaction mixture was stirred for 3 h at rt before aq NaHCO$_3$ was added. The resulting solution was extracted with CH$_2$Cl$_2$. The combined organic layer was dried over Na$_2$SO$_4$, filtered, concentrated, and the resulting residue was purified by silica gel chromatography (eluent: 10% MeOH in CH$_2$Cl$_2$), giving the product **21** as a pale-yellow oil (75%, 0.80 g). ^{1}H NMR (DMSO-*d$_6$*): δ 2.16 (s, 3H), 2.34 (m, 4H), 2.46 (m, 4H), 3.62 (s, 2H), 7.75 (d, *J* = 8.5 Hz, 1H), 8.23 (dd, *J* = 2.3, 8.5 Hz, 1H), 8.39 (d, *J* = 2.3 Hz, 1H).

A solution of **21** (0.943 g, 3.0 mmol), cyclopropaneboronic acid (0.773 g, 9.0 mmol), K$_3$PO$_4$ (2.87 g, 13.5 mmol), Pd(OAc)$_2$ (67 mg, 0.3 mmol), and tricyclohexylphosphine (0.168 g, 0.6 mmol) in toluene (15 mL) and water (3 mL) was degassed with N$_2$ and then heated at reflux overnight. Extraction followed by silica gel column chromatography (eluent: 5% NH$_3$ presaturated MeOH in CH$_2$Cl$_2$) gave the desired product **22** (0.797 g, 96%). ^{1}H NMR (CDCl$_3$): δ 0.77 (m, 2H), 1.05 (m, 1H), 2.18 (m, 1H), 2.28 (s, 3H), 2.45 (m, 4H), 2.52 (m, 4H), 3.71 (s, 2H), 7.53 (d, *J* = 8.4 Hz, 1H), 7.33 (d, *J* = 2.4 Hz, 1H), 7.98 (dd, *J* = 2.3, 8.4 Hz, 1H).

Substituted ntrobenzene **22** was completely converted into corresponding aniline **17o** after heating in MeOH at reflux for 3 h in the presence of reducing agent Fe/HOAc. The solvent was removed and the residue was partitioned between aq NaHCO$_3$ and EtOAc. Extraction, combination of organic layer, drying over Na$_2$SO$_4$, and concentration afforded essentially pure material (by HPLC). This was reacted with 3-iodo-4-methylbenzoyl chloride to furnish desired amide product **18o** in a similar fashion to the preparation of **18a**. ^{1}H NMR (DMSO-*d$_6$*): δ 0.60 (m, 2H), 0.94 (m, 2H), 2.20 (m, 1H), 2.48 (s, 3H), 2.50 (m, 8H), 3.65 (s, 2H), 7.18 (d, *J* = 8.2 Hz, 1H), 7.31 (s, 1H), 7.48 (d, *J* = 8.4 Hz, 1H), 7.65 (d, *J* = 8.4 Hz, 1H), 7.87 (d, *J* = 8.2 Hz, 1H), 8.40 (s, 1H), 10.12 (s, 1H).

General Procedure for the Preparation of Inhibitors 19 and 20: 3-[2-(Imidazo[1,2-*a*]pyridin-3-yl)ethynyl]-4-methyl-*N*-{4-[(4-methylpiperazin-1-yl)methyl]-3-(trifluoromethyl)phenyl}benzamide (19a). Alkyne **9c** (37 mg, 0.26 mmol), iodobenzamide **18a** (103.4 mg, 0.2 mmol), Pd[(PPh$_3$)$_4$] (11.6 mg, 5 mol %), and CuI (2.9 mg, 7.5 mmol%) was placed in a vial with a rubber septum. After the mixture underwent 3 cycles of vacuum/filling with N$_2$, DMF (1.5 mL) and *N,N*-diisopropylethylamine (53 µL, 0.3 mmol) was added. The mixture was then stirred at rt for 16 h. Water was added to quench the reaction, and EtOAc was added for extraction. The combined organic layer was dried (Na$_2$SO$_4$), filtered, concentrated, and the resulting residue was purified by silica gel chromatography (eluent: 5% MeOH in CH$_2$Cl$_2$, MeOH was presaturated with ammonia gas), giving the titled compound as an off-white solid (53%, 56 mg). ^{1}H NMR (DMSO-*d$_6$*): δ 2.19 (s, 3H), 2.50 (m, 8H), 2.62 (s, 3H), 3.61 (s, 2H), 7.20 (t, *J* = 6.8 Hz, 1H), 7.46 (m, 1H), 7.56 (d, *J* = 8.2 Hz,

1H), 7.72 (d, *J* = 9.4 Hz, 1H), 7.75 (d, *J* = 9.1 Hz, 1H), 7.94 (dd, *J* = 1.7, 8.0 Hz, 1H), 8.08 (s, 1H), 8.09 (d, *J* = 9.1 Hz, 1H), 8.23 (d, *J* = 1.9 Hz, 1H), 8.27 (d, *J* = 1.6 Hz, 1H), 8.63 (d, *J* = 6.7 Hz, 1H), 10.55 (s, 1H). MS: *m/z* 532.1 [M + H]$^+$.

N-{3-[2-(Imidazo[1,2-*a*]pyridin-3-yl)ethynyl]-4-methylphenyl}-4-[(4-methyl-1-piperazinyl)methyl]-3-(trifluoromethyl)benzamide (19b). This was made from the coupling of **9c** and **18b** in 20% yield. ^{1}H NMR (DMSO-*d$_6$*): δ 2.10 (s, 3H), 2.11 (s, 3H), 2.50 (m, 8H), 3.76 (s, 2H), 7.01(m, 1H), 7.22 (d, *J* = 8.4 Hz, 1H), 7.30 (m, 1H), 7.52 (m, 2H), 7.75(d, *J* = 8.2 Hz, 1H), 7.90 (s, 1H), 8.10 (m, 2H), 8.35 (d, *J* = 6.6 Hz, 1H), 10.20 (s, 1H). MS: *m/z* 532.4 [M + H]$^+$.

3-[2-(Imidazo[1,2-*a*]pyridin-3-yl)ethynyl]-4-methyl-*N*-{3-[(4-methylpiperazin-1-yl)methyl]-5-(trifluoromethyl)phenyl}benzamide (19c). This was made from the coupling of **9c** and **18c**[28] in 68% yield; characterized as HCl salt. ^{1}H NMR (D$_2$O): δ 2.35 (s, 3H), 2.41 (s, 3H), 2.64 (m, 8H), 3.71 (s, 2H), 7.30 (m, 1H), 7.52 (m, 3H), 7.90 (d, *J* = 9.0 Hz, 1H), 8.05 (dd, *J* = 1.8 Hz, 1H), 8.20 (m, 2H), 8.32 (s, 1H), 8.51(d, *J* = 1.6 Hz, 1H), 8.80 (d, *J* = 6.7 Hz, 1H), 10.60 (s, 1H). MS: *m/z* 532.0 [M + H]$^+$.

3-[2-(Imidazo[1,2-*a*]pyridin-3-yl)ethynyl]-4-methyl-*N*-[4-(4-morpholinylmethyl)-3-(trifluoromethyl)phenyl]benzamide (19d). This was made analogously to **19a** using morpholine instead of *N*-methylpiperazine in the first step S$_N$2 displacement of the reaction sequence depicted in Scheme 4. ^{1}H NMR (acetone-*d$_6$*): δ 2.46 (t, *J* = 4.5 Hz, 4H), 2.65 (s, 3H), 3.65 (m, 4H), 7.17 (t, *J* = 6.8 Hz, 1H), 7.46 (dd, *J* = 7.3, 7.7 Hz, 1H), 7.52 (d, *J* = 8.1 Hz, 1H), 7.72 (d, *J* = 8.4 Hz, 1H), 7.83 (d, *J* = 8.5 Hz, 1H), 7.97 (dd, *J* = 1.7, 8.0 Hz, 1H), 8.10 (s, 1H), 8.11 (d, *J* = 8.1 Hz, 1H), 8.24 (d, *J* = 1.5 Hz, 1H), 8.29 (s, 1H), 8.67 (d, *J* = 4.3 Hz, 1H), 9.83 (s, 1H). MS: *m/z* 518.8 [M + H]$^+$.

N-{4-[[(3S)-3-(Dimethylamino)-1-pyrrolidinyl]methyl]-3-(trifluoromethyl)phenyl}-3-[2-(imidazo[1,2-*a*]pyridin-3-yl)ethynyl]-4-methylbenzamide (19e). ^{1}H NMR (DMSO-*d$_6$*): δ 1.63 (m, 1H), 1.86 (m, 1H), 2.09 (s, 6H), 2.33 (m, 2H), 2.55 (m, 2H), 2.57 (s, 3H), 2.79 (m, 1H), 3.61 (s, 2H), 7.12 (t, *J* = 6.8 Hz, 1H), 7.40 (dd, *J* = 7.3, 7.7 Hz, 1H), 7.49 (d, *J* = 8.2 Hz, 1H), 7.67 (d, *J* = 9.1 Hz, 1H), 7.72 (d, *J* = 9.4 Hz, 1H), 7.89 (dd, *J* = 1.7, 8.0 Hz, 1H), 7.96 (d, *J* = 9.1 Hz, 1H), 7.99 (s, 1H), 8.11 (d, *J* = 1.9 Hz, 1H), 8.19 (d, *J* = 1.6 Hz, 1H), 8.58 (d, *J* = 6.7 Hz, 1H), 10.49 (s, 1H). MS: *m/z* 546.1 [M + H]$^+$.

N-{4-[(Hexahydro-4-methyl-1*H*-1,4-diazepin-1-yl)methyl]-3-(trifluoromethyl)-phenyl}-3-[2-(imidazo[1,2-*a*]pyridin-3-yl)ethynyl]-4-methylbenzamide (19f). ^{1}H NMR (DMSO-*d$_6$*): δ 1.80 (m, 2H), 2.27 (s, 3H), 2.63 (s, 3H), 2.64 (m, 8H), 3.74 (s, 2H), 7.20 (t, *J* = 6.8 Hz, 1H), 7.47 (dd, *J* = 7.3, 7.7 Hz, 1H), 7.57 (d, *J* = 8.2 Hz, 1H), 7.75 (d, *J* = 9.1 Hz, 1H), 7.80 (d, *J* = 9.4 Hz, 1H), 7.96 (dd, *J* = 1.7, 8.0 Hz, 1H), 8.03 (d, *J* = 9.1 Hz, 1H), 8.06 (s, 1H), 8.18 (d, *J* = 1.9 Hz, 1H), 8.27 (d, *J* = 1.6 Hz, 1H), 8.66 (d, *J* = 6.7 Hz, 1H), 10.56 (s, 1H). MS: *m/z* 546.1 [M + H]$^+$.

3-[2-(Imidazo[1,2-*a*]pyridin-3-yl)ethynyl]-4-methyl-*N*-{4-[(1-methyl-4-piperidinyl)oxy]-3-(trifluoromethyl)phenyl}benzamide (19g). ^{1}H NMR (CD$_3$OD): δ 1.93 (m, 2H), 2.01 (m, 2H), 2.33 (s, 3H), 2.50 (m, 2H), 2.64 (s, 3H), 2.70 (m, 2H), 4.65 (m, 1H), 7.20 (d, *J* = 8.2 Hz, 1H), 7.25 (d, *J* = 8.3 Hz, 1H), 7.49 (d, *J* = 8.0 Hz, 1H), 7.52 (d, *J* = 8.1 Hz, 1H), 7.69 (d, *J* = 8.4 Hz, 1H), 7.88 (dd, *J* = 2.0, 8.1 Hz, 2H), 7.93 (s, 1H), 8.00 (d, *J* = 2.5 Hz, 1H), 8.18 (d, *J* = 1.9 Hz, 1H), 8.56 (d, *J* = 6.8 Hz, 1H).

N-{4-[(4-Ethylpiperazin-1-yl)methyl]-3-(trifluoromethyl)phenyl}-3-[2-(imidazo[1,2-*a*]pyridin-3-yl)ethynyl]-4-methylbenzamide (19h). ^{1}H NMR (DMSO-*d$_6$*): δ 1.10 (br, 3H), 2.42 (s, 3H), 2.60 (m, 4H), 2.71 (m, 6H), 3.81 (s, 2H), 7.20 (m, 1H), 7.54 (m, 1H), 7.64 (d, *J* = 8.0 Hz, 1H), 7.72 (m, 2H), 7.91 (d, *J* = 8.0 Hz, 1H), 8.15 (m, 1H), 8.22 (m, 1H), 8.31 (m, 2H), 8.60 (d, *J* = 6.6 Hz, 1H), 10.6 (s, 1H). MS: *m/z* 546.0 [M + H]$^+$.

3-[2-(Imidazo[1,2-*a*]pyridin-3-yl)ethynyl]-4-methyl-*N*-{4-[[4-(1-methyl)ethylperazin-1-yl]methyl]-3-(trifluoromethyl)phenyl}benzamide (19i). ^{1}H NMR (DMSO-*d$_6$*): δ 1.01 (d, *J* = 6.8 Hz, 6H), 2.39 (m, 8H), 2.65 (s, 3H), 2.98 (m, 1H), 3.60 (s, 2H), 7.19 (t, *J* = 6.8 Hz, 1H), 7.47 (dd, *J* = 7.3, 7.7 Hz, 1H), 7.56 (d, *J* = 8.2 Hz, 1H), 7.74 (d, *J* = 9.1 Hz, 1H), 7.80 (d, *J* = 9.4 Hz, 1H), 7.95

(dd, J = 1.7, 8.0 Hz, 1H), 8.02 (d, J = 9.1 Hz, 1H), 8.05 (s, 1H), 8.18 (d, J = 1.9 Hz, 1H), 8.27 (d, J = 1.6 Hz, 1H), 8.65 (d, J = 6.7 Hz, 1H), 10.55 (s, 1H). MS: m/z 560.2 [M + H]$^+$.

N-{4-[(4-(2-Hydroxyethyl)piperazin-1-yl)methyl]-3-(trifluoromethyl)phenyl}-3-[2-(imidazo[1,2-a]pyridin-3-yl)ethynyl]-4-methylbenzamide (19j). ^{1}H NMR (MeOH-d_4): δ 2.41 (m, 6H), 2.55 (s, 3H), 2.80 (m, 4H), 3.62 (m, 2H), 3.83 (s, 2H), 7.20 (m, 1H), 7.41 (m, 2H), 7.65 (d, J = 9.1 Hz, 1H) 7.77 (d, J = 9.1 Hz, 1H), 7.81 (m, 3H), 8.05 (d, J = 1.9 Hz, 1H), 8.11 (d, J = 1.9 Hz, 1H), 8.55 (d, J = 6.7 Hz, 1H). MS: m/z 562.2 [M + H]$^+$.

N-{4-[(4-(2-Fluoroethyl)piperazin-1-yl)methyl]-3-(trifluoromethyl)phenyl}-3-[2-(imidazo[1,2-a]pyridin-3-yl)ethynyl]-4-methylbenzamide (19k). This was made from coupling of **9c** and **18k** in 81% yield. ^{1}H NMR (DMSO-d_6): δ 2.31 (m, 4H), 2.41 (s, 3H), 2.50 (m, 6H), 3.72 (s, 2H), 4.53 (m, 1H), 4.70 (m, 1H), 7.30 (m, 1H), 7.55 (m, 1H), 7.65 (d, J = 8.1 Hz, 1H), 7.81 (m, 2H), 8.10 (d, J = 8.1 Hz, 1H), 8.22 (m, 2H), 8.31 (s, 1H), 8.35 (s, 1H), 8.70 (d, J = 6.6 Hz, 1H), 10.3 (s, 1H). MS: m/z 564.2 [M + H]$^+$.

3-[2-(Imidazo[1,2-a]pyridin-3-yl)ethynyl]-4-methyl-N-[4-(1-piperazinylmethyl)-3-(trifluoromethyl)phenyl]benzamide (19l). This was made from coupling of **9c** and **18l** followed by standard de-Boc with TFA. ^{1}H NMR (DMSO-d_6): δ 2.33 (m, 4H), 2.62 (s, 3H), 2.72 (t, J = 4.5 Hz, 4H), 3.54 (s, 2H), 7.20 (t, J = 6.7 Hz, 1H), 7.47 (dd, J = 6.9, 8.9 Hz, 1H), 7.56 (d, J = 8.0 Hz, 1H), 7.73 (d, J = 3.9 Hz, 1H), 7.76 (d, J = 4.6 Hz, 1H), 7.94 (d, J = 7.9 Hz, 1H), 8.07 (d, J = 5.1 Hz, 1H), 8.08 (s, 1H), 8.22 (s, 1H), 8.27 (s, 1H), 8.63 (d, J = 6.6 Hz, 1H), 10.54 (s, 1H). MS: m/z 518.1 [M + H]$^+$.

3-[2-(Imidazo[1,2-a]pyridin-3-yl)ethynyl]-4-methyl-N-{4-[(3-methylpiperazin-1-yl)methyl]-3-(trifluoromethyl)phenyl}benzamide (19m). Substituted *N*-benzylpiperazine **16m** was prepared analogously to **16a** using 2-methylpiperazine instead of *N*-methylpiperazine as starting material. Coventional Boc protection (Boc$_2$O, DMAP) of **16m** gave **16m′** in 69% yield. This was converted to **18m** similarly to the synthesis of **18a** from **16a** except that the reduction of NO$_2$ to NH$_2$ was done via hydrogenation on Pd/C in 66% yield. The coupling of **9c** and **18m** followed by standard de-Boc with TFA furnished desired product, which was purified by reverse phase prep-HPLC (MeCN/H$_2$O, 0.1% TFA) as TFA salt. ^{1}H NMR (DMSO-d_6): δ 1.19 (d, J = 6.9 Hz, 3H), 2.15 (t, J = 11.2 Hz, 1H), 2.34 (t, J = 11.3 Hz, 1H), 2.62 (s, 3H), 2.84 (dd, J = 10.9, 11.7 Hz, 2H), 3.02 (d, J = 9.2 Hz, 1H), 3.28 (d, J = 10.4 Hz, 2H), 3.66 (s, 2H), 7.20 (dd, J = 6.5, 6.7 Hz, 1H), 7.48 (dd, J = 6.9, 8.1 Hz, 1H), 7.56 (d, J = 8.1 Hz, 1H), 7.73 (d, J = 7.9 Hz, 1H), 7.76 (d, J = 8.1 Hz, 1H), 7.94 (d, J = 7.9 Hz, 1H), 8.10 (s, 1H), 8.12 (d, J = 8.6 Hz, 1H), 8.25 (d, J = 9.1 Hz, 2H), 8.50 (br, 1H), 8.63 (d, J = 6.4 Hz, 1H), 8.93 (br, 1H), 10.59 (s, 1H). MS: m/z 532.2 [M + H]$^+$.

4-Methyl-N-{4-[(4-methylpiperazin-1-yl)methyl]-3-(trifluoromethyl)phenyl}-3-[2-(1H-pyrrolo[2,3-b]pyridin-5-yl)ethynyl]benzamide (20a). ^{1}H NMR (DMSO-d_6): δ 2.17 (s, 3H), 2.33 (m, 4H), 2.40 (m, 4H), 2.58 (s, 3H), 3.57 (s, 2H), 6.52 (dd, J = 1.8, 3.4 Hz, 1H), 7.52 (d, J = 8.0 Hz, 1H), 7.57 (dd, J = 2.8, 3.2 Hz, 1H), 7.71 (d, J = 8.4 Hz, 1H), 7.90 (dd, J = 1.8, 7.8 Hz, 1H), 8.07 (dd, J = 1.8, 7.8 Hz, 1H), 8.17 (d, J = 1.8 Hz, 1H), 8.22 (m, 2H), 8.45 (d, J = 2.0 Hz, 1H), 10.51 (s, 3H), 11.93 (s, 3H). MS: m/z 531.8 [M + H]$^+$.

3-[2-(3H-Imidazo[4,5-b]pyridin-6-yl)ethynyl]-4-methyl-N-{4-[(4-methylpiperazin-1-yl)methyl]-3-(trifluoromethyl)phenyl}benzamide (20b). ^{1}H NMR (CD$_2$Cl$_2$): δ 2.27 (s, 3H), 2.47 (m, 8H), 2.55 (s, 3H), 3.63 (s, 2H), 7.36 (d, J = 8.1 Hz, 1H), 7.61 (m, 1H), 7.75 (d, J = 8.5 Hz, 1H), 7.79 (m, 1H), 7.82 (dd, J = 1.8, 8.0 Hz, 1H), 7.94 (d, J = 8.8 Hz, 1H), 8.07 (dd, J = 1.8, 8.9 Hz, 1H), 8.09 (s, 1H), 8.30 (s, 1H), 8.56 (d, J = 1.6 Hz, 1H), 8.88 (br, 1H).

4-Methyl-N-{4-[(4-methylpiperazin-1-yl)methyl]-3-(trifluoromethyl)phenyl}-3-[2-(2-oxo-2,3-dihydro-1H-imidazo[4,5-b]pyridin-6-yl)ethynyl]benzamide (20c). ^{1}H NMR (DMSO-d_6): δ 2.17 (s, 3H), 2.37 (m, 8H), 2.55 (s, 3H), 3.57 (s, 2H), 7.38 (d, J = 1.4 Hz, 1H), 7.51 (d, J = 8.1 Hz, 1H), 7.71 (d, J = 8.6 Hz, 1H), 7.90 (dd, J = 1.8, 8.0 Hz, 1H), 8.06 (d, J = 8.4 Hz, 1H), 8.14 (d, J = 1.7 Hz, 2H), 8.21 (d, J = 1.8 Hz, 1H), 10.50 (s, 1H), 11.03 (s, 1H), 11.61 (s, 1H). MS: m/z 549.2 [M + H]$^+$.

4-Methyl-N-{4-[(4-methylpiperazin-1-yl)methyl]-3-(trifluoromethyl)phenyl}-3-[2-(3-oxo-3,4-dihydro-2H-pyrido[3,2-b][1,4]oxazin-7-yl)ethynyl]benzamide (20d). ^{1}H NMR (DMSO-d_6): δ 2.16 (s, 3H), 2.34 (m, 4H), 2.39 (m, 4H), 2.55 (s, 3H), 3.57 (s, 2H), 4.70 (d, J = 6.3 Hz, 2H), 7.51 (d, J = 8.2 Hz, 1H), 7.56 (d, J = 1.8 Hz, 1H), 7.71 (d, J = 8.5 Hz, 1H), 7.92 (dd, J = 1.7, 8.0 Hz, 1H), 8.06 (dd, J = 1.7, 8.5 Hz, 1H), 8.15 (d, J = 1.6 Hz, 1H), 8.16 (d, J = 1.9 Hz, 1H), 8.20 (d, J = 2.0 Hz, 1H), 10.52 (s, 1H), 11.51 (s, 1H). MS: m/z 564.1 [M + H]$^+$.

3-[2-(Imidazo[1,2-a]pyrimidin-3-yl)ethynyl]-4-methyl-N-{4-[(4-Methylpiperazin-1-yl)methyl]-3-(trifluoromethyl)phenyl}benzamide (20e). ^{1}H NMR (DMSO-d_6): δ 2.16 (s, 3H), 2.34 (m, 4H), 2.40 (m, 4H), 2.62 (s, 3H), 3.57 (s, 2H), 7.31 (dd, J = 4.2, 6.8 Hz, 1H), 7.57 (d, J = 8.2 Hz, 1H), 7.72 (d, J = 8.6 Hz, 1H), 7.95 (dd, J = 1.9, 8.0 Hz, 1H), 8.07 (dd, J = 2.0, 8.4 Hz, 1H), 8.22 (d, J = 2.0 Hz, 1H), 8.23 (s, 1H), 8.28 (d, J = 1.8 Hz, 1H), 8.67 (dd, J = 2.0, 4.1 Hz, 1H), 9.06 (dd, J = 2.0, 6.8 Hz, 1H), 10.54 (s, 1H). MS: m/z 533.2 [M + H]$^+$.

3-[2-(Imidazo[1,2-a]pyrazin-3-yl)ethynyl]-4-methyl-N-{4-[(4-methylpiperazin-1-yl)methyl]-3-(trifluoromethyl)phenyl}benzamide (20f). ^{1}H NMR (DMSO-d_6): δ 2.10 (m, 4H), 2.17 (s, 3H), 2.40 (m, 7H), 3.71 (s, 2H), 7.50 (d, J = 8.0 Hz, 1H), 7.65 (d, J = 8.0 Hz, 1H), 7.87 (d, J = 8.0 Hz, 1H), 8.00 (d, J = 8.0 Hz, 1H), 8.10 (s, 2H), 8.25 (d, J = 8.0 Hz, 1H), 8.31 (s, 1H), 8.55 (d, J = 4.4 Hz, 1H), 9.10 (s, 1H), 10.50 (s, 1H). MS: m/z 533.1 [M + H]$^+$.

3-[2-(Imidazo[1,2-b]pyridazin-3-yl)ethynyl]-4-methyl-N-{4-[(4-methylpiperazin-1-yl)methyl]-3-(trifluoromethyl)phenyl}benzamide (20g). ^{1}H NMR (DMSO-d_6): δ 2.15 (s, 3H), 2.33 (m, 4H), 2.39 (m, 4H), 2.61 (s, 3H), 3.56 (s, 2H), 7.39 (dd, J = 4.5, 9.2 Hz, 1H), 7.55 (d, J = 8.1 Hz, 1H), 7.71 (d, J = 8.5 Hz, 1H), 7.95 (dd, J = 1.9, 8.0 Hz, 1H), 8.06 (dd, J = 1.9, 8.5 Hz, 1H), 8.21 (d, J = 1.7 Hz, 2H), 8.23 (s, 1H), 8.25 (dd, J = 1.5, 9.2 Hz, 1H), 8.72 (dd, J = 1.5, 4.4 Hz, 1H), 10.54 (s, 1H). MS: m/z 533.3 [M + H]$^+$.

N-{4-[(4-Ethylpiperazin-1-yl)methyl]-3-(trifluoromethyl)phenyl}-3-[2-(imidazo[1,2-b]pyridazin-3-yl)ethynyl]-4-methylbenzamide (20h). Purified as HCl salts. ^{1}H NMR (D$_2$O): δ 1.32 (t, J = 7.2 Hz, 3H), 2.38 (s, 3H), 3.27 (q, J = 7.2 Hz, 2H), 3.28 (m, 4H), 3.48 (m, 4H), 4.15 (s, 2H), 7.26 (d, J = 8.0 Hz, 1H), 7.39 (dd, J = 4.2, 9.6 Hz, 1H), 7.56 (d, J = 8.8 Hz, 1H), 7.63 (d, J = 8.0 Hz, 1H), 7.70 (d, J = 8.8 Hz, 1H), 7.88 (d, J = 9.2 Hz, 2H), 8.02 (s, 1H), 8.09 (d, J = 9.6 Hz, 1H), 8.67 (d, J = 4.4 Hz, 1H).

N-{4-[(4-(2-Hydroxyethyl)piperazin-1-yl)methyl]-3-(trifluoromethyl)phenyl}-3-[2-(imidazo[1,2-b]pyridazin-3-yl)ethynyl]-4-methylbenzamide (20i). Purified as HCl salt. ^{1}H NMR (D$_2$O): δ 1.25 (s, 3H), 3.44 (s, 2H), 3.61 (m, 4H), 3.71 (m, 4H), 3.94 (s, 2H), 4.44 (s, 2H), 7.11 (d, J = 7.6 Hz, 1H), 7.54−7.59 (m, 3H), 7.70 (d, J = 8.0 Hz, 1H), 7.74 (s, 1H), 7.88 (s, 1H), 8.02 (s, 1H), 8.10 (d, J = 9.2 Hz, 1H), 8.70 (d, J = 2.0 Hz, 1H).

3-[2-(Imidazo[1,2-b]pyridazin-3-yl)ethynyl]-4-methyl-N-[4-(1-piperazinylmethyl)-3-(trifluoromethyl)phenyl}benzamide (20j). ^{1}H NMR (DMSO-d_6): δ 2.38 (m, 4H), 2.66 (s, 3H), 2.75 (m, 4H), 3.61 (s, 2H), 7.40 (dd, J = 4.4, 9.2 Hz, 1H), 7.58 (d, J = 8.2 Hz, 1H), 7.72 (d, J = 8.2 Hz, 1H), 7.97 (dd, J = 1.9, 8.0 Hz, 1H), 8.09 (dd, J = 2.0, 8.4 Hz, 1H), 8.15−8.31 (m, 4H), 8.77 (dd, J = 1.5, 4.4 Hz, 1H), 10.59 (s, 1H). MS: m/z 519.0 [M + H]$^+$.

3-[2-(Imidazo[1,2-b]pyridazin-3-yl)ethynyl]-N-{4-[(4-methylpiperazin-1-yl)methyl]-3-(trifluoromethyl)phenyl}benzamide (20k). ^{1}H NMR (DMSO-d_6): δ 2.17 (s, 3H), 2.37 (m, 8H), 3.57 (s, 2H), 7.40 (dd, J = 4.5, 9.2 Hz, 1H), 7.65 (t, J = 7.8 Hz, 1H), 7.72 (d, J = 8.6 Hz, 1H), 7.84 (d, J = 7.8 Hz, 1H), 8.04 (dd, J = 1.2, 9.4 Hz, 1H), 8.07 (d, J = 9.3 Hz, 1H), 8.22 (m, 1H), 8.23 (s, 1H), 8.25 (d, J = 1.6 Hz, 1H), 8.28 (d, J = 1.6 Hz, 1H), 8.73 (dd, J = 1.5, 4.4 Hz, 1H), 10.63 (s, 1H). MS: m/z 519.2 [M + H]$^+$.

4-Chloro-3-[2-(imidazo[1,2-b]pyridazin-3-yl)ethynyl]-N-{4-[(4-methylpiperazin-1-yl)methyl]-3-(trifluoromethyl)phenyl}benzamide (20l). ^{1}H NMR (DMSO-d_6): δ 2.15 (s, 3H), 2.50 (m, 4H), 2.84 (m, 4H), 3.63 (s, 2H), 7.44 (dd, J = 4.5, 9.2 Hz, 1H), 7.73 (d, J = 8.6 Hz, 1H), 7.83 (d, J = 8.5 Hz, 1H), 8.03 (dd, J = 2.2, 8.5 Hz, 1H), 8.09 (d, J = 8.5 Hz, 1H), 8.20 (d, J = 2.0 Hz, 1H),

8.28 (s, 1H), 8.29 (dd, *J* = 1.5, 9.2 Hz, 1H), 8.35 (d, *J* = 2.1 Hz, 1H), 8.74 (dd, *J* = 1.4, 4.5 Hz, 1H), 10.68 (s, 1H). MS: *m/z* 553.3 [M + H]$^+$.

4-Fluoro-3-[2-(imidazo[1,2-*b*]pyridazin-3-yl)ethynyl]-*N*-{4-[(4-methylpiperazin-1-yl)methyl]-3-(trifluoromethyl)phenyl}benzamide (20m). ^{1}H NMR (DMSO-*d*$_6$): δ 2.20 (s, 3H), 2.50 (m, 8H), 3.59 (s, 2H), 7.43 (dd, *J* = 4.5, 9.2 Hz, 1H), 7.59 (dd, *J* = 8.9, 9.1 Hz, 1H), 7.73 (d, *J* = 8.7 Hz, 1H), 8.05−8.14 (m, 2H), 8.21 (d, *J* = 2.0 Hz, 1H), 8.29 (s, 1H), 8.30 (m, 1H), 8.35 (dd, *J* = 2.2, 6.8 Hz, 1H), 8.75 (dd, *J* = 1.5, 4.4 Hz, 1H), 10.63 (s, 1H). MS: *m/z* 537.3 [M + H]$^+$.

***N*-{3-Chloro-4-[(4-methylpiperazin-1-yl)methyl]phenyl}-3-[2-(imidazo[1,2-*b*]pyridazin-3-yl)ethynyl]-4-methylbenzamide (20n).** ^{1}H NMR (DMSO-*d*$_6$): δ 2.17 (s, 3H), 2.33 (m, 4H), 2.44 (m, 4H), 2.62 (s, 3H), 3.53 (s, 2H), 7.40 (dd, *J* = 4.5, 9.2 Hz, 1H), 7.44 (d, *J* = 8.4 Hz, 1H), 7.55 (d, *J* = 8.0 Hz, 1H), 7.72 (dd, *J* = 2.1, 9.4 Hz, 1H), 7.94 (dd, *J* = 1.9, 8.0 Hz, 1H), 7.98 (d, *J* = 2.0 Hz, 1H), 8.20 (d, *J* = 1.8 Hz, 1H), 8.24 (s, 1H), 8.27 (dd, *J* = 1.5, 9.2 Hz, 1H), 8.73 (dd, *J* = 1.5, 4.4 Hz, 1H), 10.43 (s, 1H).

***N*-{3-Cyclopropyl-4-[(4-methylpiperazin-1-yl)methyl]phenyl}-3-[2-(imidazo[1,2-*b*]pyridazin-3-yl)ethynyl]-4-methylbenzamide (20o).** ^{1}H NMR (DMSO-*d*$_6$): δ 0.60 (m, 2H), 0.94 (m, 2H), 2.20 (s, 3H), 2.25 (m, 1H), 2.27−2.50 (m, 8H), 2.60 (s, 3H), 3.56 (s, 2H), 7.20 (d, *J* = 8.3 Hz, 1H), 7.34 (d, *J* = 1.9 Hz, 1H), 7.39 (dd, *J* = 4.4, 9.2 Hz, 1H), 7.53 (d, *J* = 8.2 Hz, 1H), 7.61 (d, *J* = 8.2 Hz, 1H), 7.91 (dd, *J* = 1.7, 8.2 Hz, 1H), 8.18 (d, *J* = 1.6 Hz, 1H), 8.23 (s, 1H), 8.26 (dd, *J* = 1.4, 9.2 Hz, 1H), 8.73 (dd, *J* = 1.3, 4.4 Hz, 1H), 10.16 (s, 1H).

3-[2-(Imidazo[1,2-*b*]pyridazin-3-yl)ethynyl]-4-methyl-*N*-[3-(trifluoromethyl)phenyl] Benzamide (20p). ^{1}H NMR (CDCl$_3$): δ 8.52 (d, *J* = 5.2 Hz, 1 H), 8.22 (s, 1H), 8.10 (s, 1H), 8.07 (d, *J* = 2.4 Hz, 1H), 8.04 (d, *J* = 9.2 Hz, 1H), 8.00 (s, 1H), 7.93 (d, *J* = 8.0 Hz, 1H), 7.84 (dd, *J* = 1.9, 8.0 Hz, 1 H), 7.51 (t, *J* = 8.1 Hz, 1H), 7.42 (m, 2H), 7.18 (dd, *J* = 4.8, 5.0 Hz, 1H), 2.65 (s, 3H).

3-[2-(Imidazo[1,2-*b*]pyridazin-3-yl)ethyl]-4-methyl-*N*-{4-[(4-methylpiperazin-1-yl)methyl]-3-(trifluoromethyl)phenyl}benzamide (24a). A tri-HCl salt of **20g** (400 mg) was dissolved in water (10 mL) and then subjected to hydrogenation under 28 psi for 72 h using 10% wet Pd/C (100 mg) as the catalyst. The catalyst was then removed by filtration, and the filtrate was basified to pH ∼9 with 2 M aq NaOH. Extraction with CH$_2$Cl$_2$ and silica gel column chromatography (eluent: 5% NH$_3$ presaturated MeOH in CH$_2$Cl$_2$) followed by recrystallization from EtOH gave the desired product as an off-white solid (240 mg, 70%). ^{1}H NMR (CDCl$_3$): δ 8.36 (d, *J* = 2.9 Hz, 1H), 7.95 (m, 2H), 7.89 (s, 1H), 7.74 (m, 2H), 7.61 (d, *J* = 7.9 Hz, 1H), 7.53 (s, 1H), 7.47 (s, 1H), 7.28 (d, *J* = 9.2 Hz), 7.02 (m, 1H), 3.69 (s, 2H), 3.34 (t, *J* = 7.8 Hz, 2H), 3.15 (t, *J* = 7.8 Hz, 2H), 2.67 (m, 6H), 2.48 (m, 2H), 2.42 (s, 3H), 1.27 (s, 3H). MS: *m/z* 537.4 [M + H]$^+$.

3-[2-(Imidazo[1,2-*b*]pyridazin-3-yl)vinyl]-4-methyl-*N*-{4-[(4-methylpiperazin-1-yl)methyl]-3-(trifluoromethyl)phenyl}benzamide (24b). A solution of **18a** (189.3 mg, 0.366 mmol), tributyl(vinyl)-tin (464.1 mg, 1.464 mmol), Pd$_2$(dba)$_3$·CHCl$_3$ (10 mg, 0.01 mmol), and tri(2-furyl)phosphine (18 mg, 0.074 mmol) in dry DMF (4 mL) was degassed with N$_2$ and then stirred at rt for 15 h. The solvent was evaporated, and the residue was dissolved in EtOAc. Washing with satd aq Na$_2$CO$_3$ followed by evaporation of organic solvents and silica gel column chromatography (eluent: 10% MeOH in CH$_2$Cl$_2$) gave substituted styrene **23** as a white solid (146 mg, 96%).

A suspension of **23** (146 mg, 0.35 mmol), **7d** (133 mg, 0.67 mmol), Pd(OAc)$_2$ (6.4 mg, 0.028 mmol), P(*o*-tol)$_3$ (17.4 mg, 0.057 mmol), and (*i*-Pr)$_2$NEt (0.29 mL, 1.39 mmol) in DMF (3 mL) was degassed with N$_2$ and then heated at 110 °C for 15 h. Upon cooling, the reaction mixture was dilute with CH$_2$Cl$_2$. After washing with water and evaporation of organic solvents, the residue was purified by silica gel column chromatography (eluent: 5% NH$_3$ presaturated MeOH in CH$_2$Cl$_2$), giving a dark-brown solid. Recrystallization from CHCl$_3$/ether afforded an off-white solid (50 mg, 25%). ^{1}H NMR (CDCl$_3$): δ 8.46 (d, *J* = 3.0 Hz, 1H), 8.20 (d, *J* = 1.3 Hz, 1H), 8.06 (s, 1H), 8.04 (m, 1H), 8.02−7.97 (m, 2H), 7.93−7.86 (m, 2H), 7.69 (d, *J* = 8.4 Hz, 1H),

7.49 (d, *J* = 16.8 Hz, 1H), 7.35 (d, *J* = 7.6 Hz, 1H), 7.10 (t, *J* = 4.5 Hz, 1H), 3.76 (s, 2H), 2.87 (br, 6H), 2.70 (br, 2H), 2.56 (s, 3H), 1.56 (s, 3H). MS: *m/z* 535.4 [M + H]$^+$.

Modeling Studies. The binding site model used for Abl docking was based on the X-ray coordinates of Abl bound with imatinib (PDB: 1IEP). Protein side chains within a 5 Å radius of the bound ligand were allowed to relax to optimize binding interactions using the Induced Fit protocol in the Schrodinger package.[45] Docking studies were performed with Glide in the Schrodinger modeling package.[45] The solution with the best docking score was chosen and used for analysis.

Biological Characterization of Compounds. In vitro kinase assays were carried out in-house as previously described.[21a] This assay configuration differed from that used in our previous publication on **20g**,[20] which was a commercial assay from Reaction Biology Corporation.[43] Cellular proliferation assays were performed as previously described,[21a] independently of the data set previously reported for **20g**.[20] Pharmacokinetic analyses[21a] and in vivo efficacy studies[20] were carried out according to previously published procedures.

References

(1) Quintas-Cardama, A.; Cortes, J. Molecular biology of *bcr-abl1*-positive chronic myeloid leukemia. *Blood* **2009**, *113*, 1619–1630.

(2) (a) Druker, B. J.; Tamura, S.; Buchdunger, E.; Ohno, S.; Segal, G. M.; Fanning, S.; Zimmermann, J.; Lydon, N. B. Effects of a selective inhibitor of the Abl tyrosine kinase on the growth of Bcr-Abl positive cells. *Nature Med.* **1996**, *2*, 561–566. (b) Capdeville, R.; Buchdunger, E.; Zimmermann, J.; Matter, A. Glivec (STI571, imatinib), a rationally developed, targeted anticancer drug. *Nat. Rev. Drug Dis.* **2002**, *1*, 493–502.

(3) Quintas-Cardama, A.; Kantarjian, H.; Cortes, J. Imatinib and beyond—exploring the full potential of targeted therapy for CML. *Nat. Rev. Clin. Oncol.* **2009**, *6*, 535–543.

(4) Druker, B. J.; Guilhot, F.; O'Brien, S. G.; Gathmann, I.; Kantarjian, H.; Gattermann, N.; Deininger, M. W.; Silver, R. T.; Goldman, J. M.; Stone, R. M.; Cervantes, F.; Hochhaus, A.; Powell, B. L.; Gabrilove, J. L.; Rousselot, P.; Reiffers, J.; Cornelissen, J. J.; Hughes, T.; Agis, H.; Fischer, T.; Verhoef, G.; Shepherd, J.; Saglio, G.; Gratwohl, A.; Nielsen, J. L.; Radich, J. P.; Simonsson, B.; Taylor, K.; Baccarani, M.; So, C.; Letvak, L.; Larson, R. A. Five-year follow-up of patients receiving imatinib for chronic myeloid leukemia. *N. Engl. J. Med.* **2006**, *355*, 2408–2417.

(5) O'Hare, T.; Eide, C. A.; Deininger, M. W. BCR-ABL kinase domain mutations, drug resistance, and the road to a cure for chronic myeloid leukemia. *Blood* **2007**, *110*, 2242–2249.

(6) Weisberg, E.; Manley, P. W.; Cowan-Jacob, S. W.; Hochhaus, A.; Griffin, J. D. Second generation inhibitors of BCR-ABL for the treatment of imatinib-resistant chronic myeloid leukaemia. *Nat. Rev. Cancer* **2007**, *7*, 345–356.

(7) Weisberg, E.; Manley, P. W.; Breitenstein, W.; Brueggen, J.; Cowan-Jacob, S. W.; Ray, A.; Huntly, B.; Fabbro, D.; Fendrich, G.; Hall-Meyers, E.; Kung, A. L.; Mestan, J.; Daley, G. Q.; Callahan, L.; Catley, L.; Cavazza, C.; Mohammed, A.; Neuberg, D.; Wright, R. D.; Gilliland, D. G.; Griffin, J. D. Characterization of AMN107, a selective inhibitor of native and mutant Bcr-Abl. *Cancer Cell* **2005**, *7*, 129–141.

(8) Kimura, S.; Naito, H.; Segawa, H.; Kuroda, J.; Yuasa, T.; Sato, K.; Yokota, A.; Kamitsuji, Y.; Kawata, E.; Ashihara, E.; Nakaya, Y.; Naruoka, H.; Wakayama, T.; Nasu, K.; Asaki, T.; Niwa, T.; Hirabayashi, K.; Maekawa, T. NS-187, a potent and selective dual Bcr-Abl/Lyn tyrosine kinase inhibitor, is a novel agent for imatinib-resistant leukemia. *Blood* **2005**, *106*, 3948–3954.

(9) (a) Shah, N. P.; Tran, C.; Lee, F. Y.; Chen, P.; Norris, D.; Sawyers, C. L. Overriding imatinib resistance with a novel Abl kinase inhibitor. *Science* **2004**, *305*, 399–401. (b) Lombardo, L. J.; Lee, F. Y.; Chen, P.; Norris, D.; Barrish, J. C.; Behnia, K.; Castaneda, S.; Cornelius, L. A. M.; Das, J.; Doweyko, A. M.; Fairchild, C.; Hunt, J. T.; Inigo, I.; Johnston, K.; Kamath, A.; Kan, D.; Klei, H.; Marathe, P.; Pang, S.; Peterson, R.; Pitt, S.; Schieven, G. L.; Schmidt, R. J.; Tokarski, J.; Wen, M.-L.; Wityak, J.; Borzilleri, R. M. Discovery of N-(2-chloro-6-methyl-phenyl)-2-(6-(4-(2-hydroxyethyl)-piperazin-1-yl)-2-methyl-pyrimidin-4-ylamino)thiazole-5-carboxamide (BMS - 354825), a dual Src/Abl kinase inhibitor with potent antitumor activity in preclinical assays. *J. Med. Chem.* **2004**, *47*, 6658–6661.

(10) (a) Boschelli, D. H.; Ye, F.; Wang, Y. D.; Dutia, M.; Johnson, S. L.; Wu, B.; Miller, K.; Powell, D. W.; Yaczko, D.; Young, M.; Tischler,

Huang et al.

M.; Arndt, K.; Discafani, C.; Etienne, C.; Gibbons, J.; Grod, J.; Lucas, J.; Weber, J. M.; Boschelli, F. Optimization of 4-phenyl-amino-3-quinolinecarbonitriles as potent inhibitors of Src kinase activity. *J. Med. Chem.* **2001**, *44*, 3965–3977. (b) Puttini, M.; Coluccia, A. M.; Boschelli, F.; Cleris, L.; Marchesi, E.; Donella-Deana, A.; Ahmed, S.; Redaelli, S.; Piazza, R.; Magistroni, V.; Andreoni, F.; Scapozza, L.; Formelli, F.; Gambacorti-Passerini, C. In vitro and in vivo activity of SKI-606, a novel Src-ABL inhibitor, against imatinib-resistant BCR-ABL+ neoplastic cells. *Cancer Res.* **2006**, *66*, 11314–11322.

(11) O'Hare, T.; Walters, D. K.; Stoffregen, E. P.; Jia, T.; Manley, P. W.; Mestan, J.; Cowan-Jacob, S. W.; Lee, F. Y.; Heinrich, M. C.; Deininger, M. W.; Druker, B. J. In vitro activity of BCR-ABL inhibitors AMN107 and BMS-354825 against clinically relevant imatinib-resistant ABL kinase domain mutants. *Cancer Res.* **2005**, *65*, 4500–4505.

(12) (a) Deguchi, Y.; Kimura, S.; Ashihara, E.; Niwa, T.; Hodohara, K.; Fujiyama, Y.; Maekawa, T. Comparison of imatinib, dasatinib, nilotinib and INNO-406 in imatinib-resistant cell lines. *Leuk. Res.* **2008**, *32*, 980–983. (b) Redaelli, S.; Piazza, R.; Rostagno, R.; Magistroni, V.; Perini, P.; Marega, M.; Gambacorti-Passerini, C.; Boschelli, F. Activity of bosutinib, dasatinib, and nilotinib against 18 imatinib-resistant BCR/ABL mutants. *J. Clin. Oncol.* **2009**, *27*, 469–471.

(13) (a) O'Hare, T.; Eide, C. A.; Deininger, M. W. New BCR-ABL inhibitors in chronic myeloid leukemia: keeping resistance in check. *Expert Opin. Invest. Drugs* **2008**, *17*, 865–878. (b) Tanaka, R.; Kimura, S. ABL tyrosine kinase inhibitors for overriding BCR-ABL/T315I: from the second to third generation. *Exp. Rev. Anticancer Ther.* **2008**, *8*, 1387–1398. (c) Noronha, G.; Cao, J.; Chow, C. P.; Dneprovskaia, E.; Fine, R. M.; Hood, J.; Kang, X.; Klebansky, B.; Lohse, D.; Mak, C. C.; McPherson, A.; Palanki, M. S. S.; Pathak, V. P.; Renick, J.; Soll, R.; Zeng, B. Inhibitors of ABL and the ABL-T315I mutation. *Curr. Top. Med. Chem* **2008**, *8*, 905–921. (d) Quintas-Cardama, A.; Cortes, J. Therapeutic options against BCR-ABL1 T315I-positive chronic myelogenous leukemia. *Clin. Cancer Res.* **2008**, *14*, 4392–4399.

(14) Zhou, T.; Parillon, L.; Li, F.; Wang, Y.; Keats, J.; Lamore, S.; Xu, Q.; Shakespeare, W.; Dalgarno, D.; Zhu, X. Crystal structure of the T315I mutant of Abl kinase. *Chem. Biol. Drug Des.* **2007**, *70*, 171–181.

(15) Chow, C. P.; Cao, J.; Dneprovskaia, E.; Fine, R. M.; Hanna, E.; Hood, J.; Hwang, K.; Kang, X.; Klebansky, B.; Lohse, D.; Mak, C. C.; McPherson, A.; Noronha, G.; Palanki, M. S.; Pathak, V. P.; Renick, J.; Soll, R.; Zeng, B.; Zhu, H. Design and SAR of thiazole-based inhibitors for the ABL-T315I enzyme. 234th ACS National Meeting, Boston, MA, August 19−23, 2007, Abstract MED-358.

(16) Giles, F. J.; Cortes, J.; Jones, D.; Bergstrom, D.; Kantarjian, H.; Freedman, S. J. MK-0457, a novel kinase inhibitor, is active in patients with chronic myeloid leukemia or acute lymphocytic leukemia with the T315I BCR-ABL mutation. *Blood* **2007**, *109*, 500–502.

(17) Gontarewicz, A.; Balabanov, S.; Keller, G.; Colombo, R.; Graziano, A.; Pesenti, E.; Benten, D.; Bokemeyer, C.; Fiedler, W.; Moll, J.; Brummendorf, T. H. Simultaneous targeting of Aurora kinases and BCR-ABL kinase by the small molecule inhibitor PHA-739358 is effective against imatinib-resistant BCR-ABL mutations including T315I. *Blood* **2008**, *111*, 4355–4364.

(18) Howard, S.; Berdini, V.; Boulstridge, J. A.; Carr, M. G.; Cross, D. M.; Curry, J.; Devine, L. A.; Early, T. R.; Fazal, L.; Gill, A. L.; Heathcote, M.; Maman, S.; Matthews, J. E.; McMenamin, R. L.; Navarro, E. F.; O'Brien, M. A.; O'Reilly, M.; Rees, D. C.; Reule, M.; Tisi, D.; Williams, G.; Vinkovic, M.; Wyatt, P. G. Fragment-based discovery of the pyrazol-4-yl urea (AT9283), a multitargeted kinase inhibitor with potent aurora kinase activity. *J. Med. Chem.* **2009**, *52*, 379–388.

(19) Shiotsu, Y.; Kiyoi, H.; Ishikawa, Y.; Tanizaki, R.; Shimizu, M.; Umehara, H.; Ishii, K.; Mori, Y.; Ozeki, K.; Minami, Y.; Abe, A.; Maeda, H.; Akiyama, T.; Kanda, Y.; Sato, Y.; Akinaga, S.; Naoe, T. KW-2449, a novel multi-kinase inhibitor, suppresses the growth of leukemia cells with FLT3 mutations or T315I-mutated BCR/ABL translocation. *Blood* **2009**, *114*, 1607–1617.

(20) O'Hare, T.; Shakespeare, W. C.; Zhu, X.; Eide, C. A.; Rivera, V. M.; Wang, F.; Adrian, L. T.; Zhou, T.; Huang, W.-S.; Xu, Q.; Metcalf, C. A.; Tyner, J. W.; Loriaux, M. M.; Corbin, A. S.; Wardwell, S.; Ning, Y.; Keats, J. A.; Wang, Y.; Sundaramoorthi, R.; Thomas, M.; Zou, D.; Snodgrass, J.; Commodore, L.; Sawyer, T. K.; Dalgarno, D. C.; Deininger, M. W. N.; Druker, B. J.; Clackson, T. AP24534, a pan-BCR-ABL inhibitor for chronic myeloid leukemia, potently inhibits the T315I mutant and overcomes mutation-based resistance. *Cancer Cell* **2009**, *16*, 401–412.

(21) (a) Huang, W.-S.; Zhu, X.; Wang, Y.; Azam, M.; Wen, D.; Sundaramoorthi, R.; Thomas, R. M.; Liu, S.; Banda, G.; Lentini, S. P.; Das, S.; Xu, Q.; Keats, J.; Wang, F.; Wardwell, S.; Ning, Y.;

Snodgrass, J. T.; Broudy, M. I.; Russian, K.; Daley, G. Q.; Iuliucci, J.; Dalgarno, D. C.; Clackson, T.; Sawyer, T. K.; Shakespeare, W. C. 9-(Arenethenyl)purines as dual Src/ABL kinase inhibitors targeting the inactive conformation: design, synthesis, and biological evaluation. *J. Med. Chem.* **2009**, *52*, 4743–4756. (b) Zhou, T.; Parillon, L.; Huang, W.-S.; Wang, Y.; Sawyer, T. K.; Shakespeare, W. C.; Clackson, T.; Zhu, X.; Dalgarno, D. C. Structural analysis of DFG-in and DFG-out dual Src-Abl inhibitors sharing a common vinyl purine template. *Chem. Biol. Drug Des.* **2010**, *75*, 18–28. (c) Azam, M.; Powers, J. T.; Einhorn, W.; Huang, W.-S.; Shakespeare, W. C.; Zhu, X.; Dalgarno, D. C.; Clackson, T.; Sawyer, T. K.; Daley, G. Q. AP24163 inhibits the gatekeeper mutant of BCR-ABL and suppress in vitro resistance. *Chem. Biol. Drug Des.* **2010**, *75*, 223–227.

(22) Joshi, R. V.; Xu, Z.-Q.; Ksebati, M. B.; Kessel, D.; Corbett, T. H.; Drach, J. C.; Zemlicka, J. Synthesis, transformations and biological activity of chloro enamines and ynamines derived from chloroalkenyl- and alkynyl-N-substituted purine and pyrimidine bases of nucleic acids. *J. Chem. Soc., Perkin Trans. 1* **1994**, 1089–1098.

(23) Chinchilla, R.; Najera, C. The Sonogashira reaction: a booming methodology in synthetic organic chemistry. *Chem. Rev.* **2007**, *107*, 874–922.

(24) Hand, E.; Smakula, P.; William, W. Teleamination of the imidazo-[1,2-*a*]pyridine system. *J. Org. Chem.* **1978**, *43*, 2900–2906.

(25) Huang, W.-S.; Shakespeare, W. C. An efficient synthesis of nilotinib (AMN107). *Synthesis* **2007**, 2121–2124.

(26) Ding, Q.; Gray, N. S.; Li, B.; Liu, Y.; Sim, T.; Uno, T.; Zhang, G.; Pissot-Soldermann, C.; Breitenstein, W.; Bold, G.; Caravatti, G.; Furet, P.; Guagnano, V.; Lang, M.; Manley, P. W.; Schoepfer, J.; Spanka, C. Preparation of pyrimidine urea derivatives as kinase inhibitors for use against proliferative diseases. PCT Int. Appl. WO 2006000420, 2006.

(27) Bold, G.; Caravatti, G.; Floersheimer, A.; Guagnano, V.; Imbach, P.; Masuya, K.; Roesel, J.; Vaupel, A.; Garcia-Echeverria, C. Diaryl urea derivatives, particularly N-[4-(pyrimidin-4-yloxy)phe-nyl]-N′-phenylureas, useful in the treatment of protein kinase dependent diseases, especially neoplasm, and their preparation. PCT Int. Appl. WO 2005051366, 2005.

(28) Chaffee, S. C.; Albrecht, B. K.; Hodous, B. L.; Martin, M. W.; McGowan, D. C.; Dimauro, E. F.; Reddy, G.; Cee, V. J.; Olivieri, P. R.; Reed, A.; Romero, K. Heteroaryl-substituted alkyne compounds as protein kinase inhibitors, their preparation, pharmaceutical compositions, and use in therapy. PCT Int. Appl. WO 2006044823, 2006.

(29) Modugno, M.; Casale, E.; Soncini, C.; Rosettani, P.; Colombo, R.; Lupi, R.; Rusconi, L.; Fancelli, D.; Carpinelli, P.; Cameron, A. D.; Isacchi, A.; Moll, J. Crystal structure of the T315I ABL mutant in complex with the aurora kinases inhibitor PHA-739358. *Cancer Res.* **2007**, *67*, 7987–7990.

(30) Schindler, T.; Bornmann, W.; Pellicena, P.; Miller, W. T.; Clarkson, B.; Kuriyan, J. Structural mechanism for STI-571 inhibition of abelson tyrosine kinase. *Science* **2000**, *289*, 1938–1942.

(31) Corbin, A. S.; Buchdunger, E.; Pascal, F.; Druker, B. J. Analysis of the structural basis of specificity of inhibition of the ABL kinase by STI571. *J. Biol. Chem.* **2002**, *277*, 32214–32219.

(32) Azam, M.; Latek, R. R.; Daley, G. Q. Mechanisms of autoinhibition and STI-571/imatinib resistance revealed by mutagenesis of BCR-ABL. *Cell* **2003**, *112*, 831–843.

(33) Huang, W.-S.; Wang, Y.; Sundaramoorthi, R.; Thomas, R. M.; Wen, D.; Liu, S.; Lentini, S. P.; Das, S.; Banda, G.; Sawyer, T. K.; Shakespeare, W. C. Facile synthesis of 9-(arenethenyl)purines via Heck reaction of 9-vinylpurines and aryl halides. *Tetrahedron Lett.* **2007**, *48*, 7388–7391.

(34) Nagar, B.; Bornmann, W. G.; Pellicena, P.; Schindler, T.; Veach, D. R.; Miller, W. T.; Clarkson, B.; Kuriyan, J. Crystal structures of the kinase domain of c-Abl in complex with the small molecule inhibitors PD173955 and imatinib (STI-571). *Cancer Res.* **2002**, *62*, 4236–4243.

(35) Horio, T.; Hamasaki, T.; Inoue, T.; Wakayama, T.; Itou, S.; Naito, H.; Asaki, T.; Hayase, H.; Niwa, T. Structural factors contributing to the Abl/Lyn dual inhibitory activity of 3-substituted benzamide derivatives. *Bioorg. Med. Chem. Lett.* **2007**, *17*, 2712–2717.

(36) Daylight Chemical Information System, Inc. http://www.daylight.com. Accessed November 2005.

(37) Zimmermann, J.; Buchdunger, E.; Mett, H.; Meyer, T.; Lydon, N. B. Potent and selective inhibitors of the ABL-kinase: phenyla-minopyrimidine (PAP) derivatives. *Bioorg. Med. Chem. Lett.* **1997**, *7*, 187–192.

(38) Porkka, K.; Koskenvesa, P.; Lundan, T.; Rimpilainen, J.; Mustjoki, S.; Smykla, R.; Wild, R.; Luo, R.; Arnan, M.; Brethon, B.; Eccersley, L.; Hjorth-Hansen, H.; Hoglund, M.; Klamova, H.; Knutsen, H.;

Parikh, S.; Raffoux, E.; Gruber, F.; Brito-Babapulle, F.; Dombret, H.; Duarte, R. F.; Elonen, E.; Paquette, R.; Zwaan, C. M.; Lee, F. Y. F. Dasatinib crosses the blood−brain barrier and is an efficient therapy for central nervous system Philadelphia chromosome-positive leukemia. *Blood* **2008**, *112*, 1005–1012.

(39) Yokota, A.; Kimura, S.; Masuda, S.; Ashihara, E.; Kuroda, J.; Sato, K.; Kamitsuji, Y.; Kawata, E.; Deguchi, Y.; Urasaki, Y.; Terui, Y.; Ruthardt, M.; Ueda, T.; Hatake, K.; Inui, K.-i.; Maekawa, T. INNO-406, a novel BCR-ABL/Lyn dual tyrosine kinase inhibitor, suppresses the growth of Ph+ leukemia cells in the central nervous system, and cyclosporine A augments its in vivo activity. *Blood* **2007**, *109*, 306–314.

(40) Hughes, T.; Saglio, G.; Branford, S.; Soverini, S.; Kim, D.-W.; Muller, M. C.; Martinelli, G.; Cortes, J.; Beppu, L.; Gottardi, E.; Kim, D.; Erben, P.; Shou, Y.; Haque, A.; Gallagher, N.; Radich, J.; Hochhaus, A. Impact of baseline BCR-ABL mutations on response to nilotinib in patients with chronic myeloid leukemia in chronic phase. *J. Clin. Oncol.* **2009**, *27*, 4204–4210.

(41) For other examples using the acetylene linker in kinase inhibitor design: (a) Cee, V. J.; Albrecht, B. K.; Geuns-Meyer, S.; Hughes, P.; Bellon, S.; Bready, J.; Caenepeel, S.; Chaffee, S. C.; Coxon, A.; Emery, M.; Fretland, J.; Gallant, P.; Gu, Y.; Hodous, B. L.; Hoffman, D.; Johnson, R. E.; Kendall, R.; Kim, J. L.; Long, A. M.; McGowan, D.; Morrison, M.; Olivieri, P. R.; Patel, V. F.; Polverino, A.; Powers, D.; Rose, P.; Wang, L.; Zhao, H. Alkynylpyrimidine amide derivatives as potent, selective, and orally active inhibitors of Tie-2 kinase. *J. Med. Chem.* **2007**, *50*, 627–640. (b) Hartung, I.; Bothe, U.; Kettschau, G.; Luecking, U.; Mengel, A.; Krueger, M.; Thierauch, K. H.; Lienau, P; Boemer, U. Alkynylpyrimidines as Tie2 kinase inhibitors. PCT Int. Appl. WO 2008155140, 2008. (c) Jones, C. D.; Luke, R. W. A.; Mccoull, W. Preparation of ethynylpyrimidine derivatives as Tie2 receptor tyrosine kinase inhibitors for the treatment of cancer. PCT Int. Appl. WO 2006103449, 2006. (d) Askew, B. C.; Brugger, N.; Lan, R.; Sutton, A. Pyrrolopyridine and thienopyrimidine derivatives as protein kinase inhibitors useful in the treatment of various diseases and their preparation. PCT Int. Appl. WO 2009094123, 2009. (e) Vaisburg, A.; Moradei, O.; Frechette, S.; Saavedra, O.; Isakovic, L.; Raeppel, S.; Gaudette, F. Preparation of inhibitors of kinase activity with 1,2-di-cyclyl substituted alkynes. PCT Int. Appl. WO 2009100536, 2009.

(42) NCT00660920, http://www.clinicaltrials.gov. Accessed January 2010.

(43) Reaction Biology Corporation, http://www.reactionbiology.com. Accessed August 2009.

(44) Quan, M. L.; Lam, P. Y. S.; Han, Q.; Pinto, D. J. P.; He, M. Y.; Li, R.; Ellis, C. D.; Clark, C. G.; Teleha, C. A.; Sun, J.-H.; Alexander, R. S.; Bai, S.; Luettgen, J. M.; Knabb, R. M.; Wong, P. C.; Wexler, R. R. Discovery of 1-(3′-Aminobenzisoxazol-5′-yl)-3-trifluoro-methyl-*N*-[2-fluoro-4- [(2′-dimethylaminomethyl)imidazol-1-yl]phe-nyl]-1*H*-pyrazole-5-carboxyamide Hydrochloride (Razaxaban), a Highly Potent, Selective, and Orally Bioavailable Factor Xa In-hibitor. *J. Med. Chem.* **2005**, *48*, 1729–1744.

(45) Sherman, W.; Day, T.; Jacobson, M. P.; Friesner, R. A.; Farid, R. Novel procedure for modeling ligand/receptor induced fit effects. *J. Med. Chem.* **2006**, *49*, 534–553.